Numer. Math. Theor. Meth. Appl.
doi: 10.4208/nmtma.2016.y14020

Vol. **9**, No. 3, pp. 383-415
August 2016

Spline Surfaces over Arbitrary Topological Meshes: Theoretical Analysis and Application

Chaoyang Liu[1,*] and Xiaoping Zhou[2]

[1] *School of Mathematics & Statistics, Zhengzhou University, Zhengzhou 450001, China.*
[2] *School of Information Engineering, Zhengzhou University, Zhengzhou 450001, China.*

Received 17 September 2014; Accepted 31 October 2015

Abstract. Based on polyhedral splines, some multivariate splines of different orders with given supports over arbitrary topological meshes are developed. Schemes for choosing suitable families of multivariate splines based on pre-given meshes are discussed. Those multivariate splines with inner knots and boundary knots from the related meshes are used to generate rational spline shapes with related control points. Steps for up to C^2-surfaces over the meshes are designed. The relationship among the meshes and their knots, the splines and control points is analyzed. To avoid any unexpected discontinuities and get higher smoothness, a heart-repairing technique to adjust inner knots in the multivariate splines is designed.

With the theory above, bivariate C^1-quadratic splines over rectangular meshes are developed. Those bivariate splines are used to generate rational C^1-quadratic surfaces over the meshes with related control points and weights. The properties of the surfaces are analyzed. The boundary curves and the corner points and tangent planes, and smooth connecting conditions of different patches are presented. The C^1-continuous connection schemes between two patches of the surfaces are presented.

AMS subject classifications: 65D18, 68U05

Key words: Polyhedral spline, inner knot, multivariate spline, control point, spline shape, C^k-surface, arbitrary topological mesh , rational bivariate quadratic surface, rectangular mesh.

1. Introduction

Surfaces with arbitrary topology play an important role in computer aided geometric design. Subdivision surfaces, as the main surfaces with arbitrary topology, are usually continuous and can be C^1-continuous as limiting results, with skillful subdivision methods. As limiting results, those subdivision surfaces in game design are superior to those in other designs where precision coordinates are necessary.

*Corresponding author. *Email addresses:* lcy@zzu.edu.cn (C.-Y. Liu), iexpzhou@zzu.edu.cn (X.-P. Zhou)

 ©2016 Global-Science Press

https://doi.org/10.4208/nmtma.2016.y14020 Published online by Cambridge University Press

Spline surfaces are another kind of surfaces. In 1946, Schoenberg set up the theory of univariate spline. With this theory, B-spline has been used widespreadly in [1-4], and NURBS curves became some of the most popular curves in computer aided geometric design. These successes stimulated various ideas and methods that surfaces could be designed similarly.

As tensor surfaces, NURBS surfaces are in form of tensor product of two univariate splines along two coordinates. And C^1-NURBS surfaces are rational piecewise polynomials of degree 4. Triangular Bézier surfaces are designed by generalizing Bézier curves with barycentric coordinates in the plane. Bézier curves is only a certain form of B-spline curves, however.

Naturally, bivariate splines can be directly used to design surfaces. Based on different ideas and rules, there are plenty of splines, such as simplex splines, box splines, half box splines and cone splines, or in general, polyhedral splines which are presented in [5] by Goodman (See [5] and its references for more details). With those splines over specific meshes, there are some related spline surfaces, such as box spline surfaces, *etc*.

For surfaces related to splines over arbitrary topological meshes, methods with specific techniques seem necessary. Starting with bivariate 3-directional quartic box spline, [6] proposed an algorithm for C^1-surfaces over arbitrary triangular control meshes. [7] introduced an algorithm for creating smooth spline surfaces over control triangular meshes capable of outlining arbitrary free-form surfaces with or without boundary. The resulting surface had a degree 4 parametric polynomial representation and was represented as a network of tangent plane continuous triangular Bézier patches. In [8], based on the generalized B-spline blending functions and G^1-continuous conditions, the blending matrices were derived. By means of the blending matrices, the control vertices in an irregular control polyhedron were converted to control points of piecewise B-spline patches.

A new scheme for constructing splines and spline surfaces with arbitrary topology was discussed. The second section reviewed the definition and basic properties of polyhedral splines in [5] and developed a definition of multivariate splines with given supports as well as concepts of boundary knots, inner knots and rational spline shapes, and analyzed the relationships among meshes, splines, knots, and control points. In the third section, C^0- and C^1-bivariate spline hybrid mesh surfaces were reviewed with degrees of one and two, respectively. To avoid some unexpected discontinuities and to get higher smoothness, a heart-repairing technique to adjust inner knots in the multivariate splines was designed in the fourth section. The fifth section was devoted to bivariate cubic splines and C^2-surfaces over arbitrary triangular meshes.

Based on the theory in sections from 2 to 5, bivariate quadratic C^1 splines over rectangular meshes were computed in [12]. With those splines, rational quadratic C^1-surfaces over rectangular meshes was developed.

In the sixth section, rational bivariate quadratic C^1-spline surfaces over rectangular meshes was presented. These surfaces are composed of patches. The formulas of the patches with local coordinates, related control points and weights were devel-

https://doi.org/10.4208/nmtma.2016.y14020 Published online by Cambridge University Press

oped. In the seventh section, bivariate C^1-quadratic splines over rectangular meshes were computed and analysed. The boundary curves and tangent vectors of the bivariate quadratic patches were discussed in the eighth section, and smooth connecting conditions of different patches are presented. The ninth section was devoted to the positions and tangent vectors as well as the tangent planes at the corners of the bivariate quadratic patches. In the tenth section, schemes for C^1-connection between two patches was discussed.

2. Inner knot splines and rational blending shapes

Let us present basic concepts about polyhedral splines.

2.1. Polyhedral splines

After the geometric construction to splines with simplex in $\mathbb{R}^{k+s}$, [5] presented the following definition.

Definition 2.1. *(Definition for a polyhedral spline) For $s > 1$ and $k > 0$, let P be a convex polyhedron in $\mathbb{R}^{k+s}$ and L a linear map from $\mathbb{R}^{k+s}$ to $\mathbb{R}^s$. Then the polyhedral spline $B = B_P(.|L)$ is given by*

$$B(x) = vol_k(P \bigcap L^{-1}(x)),\ x \in \mathbb{R}^s. \tag{2.1}$$

By Definition 2.1, the support for this polyhedral spline is

$$supp(B) = L(P). \tag{2.2}$$

Usually, L can be $\mathbb{R}_s$, the restriction to the first s components:

$$R_s(x_1, ..., x_s, x_{s+1}, ..., x_{s+k}) = (x_1, ..., x_s), \tag{2.3}$$

an orthogonal projection from $\mathbb{R}^{k+s}$ to $\mathbb{R}^s$.

With different convex polyhedrons, there are different kinds of splines. A few well-known examples are box splines, half-box splines, simplex splines and cone splines with related convex polyhedrons in planar or higher dimensional spaces.

As described in [5], $B_P(x|L)$ is a spline, and satisfies Lemma 2.1.

Lemma 2.1. *(Basic lemma for a polyhedron spline) A polyhedron spline $B_P(x|L)$ with*

$$P \subset \mathbb{R}^{s+k},\ L : \mathbb{R}^{s+k} \to \mathbb{R}^s,\ vol_s(L(P)) > 0 \tag{2.4}$$

is a piecewise polynomial of degree k with discontinuities only across convex sets C of dimension $s-1$ of the form $L(F)$ where F is a face of P. To be precise, if C has dimension $s-1$ and d is the maximum dimension of a face F such that $C = L(F)$, then $B_P(x|L)$ has continuous derivatives of order $k+s-d-2$ across C.

https://doi.org/10.4208/nmtma.2016.y14020 Published online by Cambridge University Press

By Lemma 2.1, it is easy to see that $s-1 \leq d$, hence,

$$k+s-d-2 \leq k-1$$

compared to the discontinuity property of univariate spline in case of repeated knots.

With univariate splines, the term 'repeated knot' means that a knot's value consecutively appears in knot-sequence of a spline whereas with multivariate splines, it does that at least $s+1$ knots are in $s-1$ dimensional space. For $s=2$ or bivariate splines, it does that at least 3 knots are colinear whether the knots' values are equal or not.

2.2. Multivariate splines with given supports

By the polyhedral spline above, there is a tendency that a spline in a certain dimensional space (where its support lie) is usually generated with a polyhedron in a higher dimensional space. And as indicated in Definition 2.1 and formula (2.2), the support is described as the image of the related polyhedron. Box splines, simplex splines and cone splines mentioned above can be defined this way (see [5], for example). And the meshes related to those splines are unique choices, $i.e.$ the meshes are the results of the polyhedrons and are unchangeable.

In fact, a mesh may exist first. A family of splines now should be chosen based on the given mesh. And some splines have to exist in specific domains, *i.e.* given supports from the mesh. In view of this point, a proper polyhedron related to a given support should be constructed if a multivariate spline with the given support is in demand. Follow some concepts for this purpose.

Definition 2.2. *(Definition for an inner convex set) Let an s-dimensional closed set $D \subset \mathbb{R}^s$ and $\{s_1, \cdots, s_k\} \subseteq D$ satisfying*
1) $[s_1, \cdots, s_k]$, the convex hull of $\{s_1, \cdots, s_k\}$, is contained in D;
2) A line segment with an end in $[s_1, \cdots, s_k]$ and another in D is contained in D.
With those requirements, $\{s_1, \cdots, s_k\}$ forms an inner convex set of D.

Lemma 2.2. *If D is convex and $\{s_1, \cdots, s_k\} \subseteq D$, $\{s_1, \cdots, s_k\}$ is always an inner convex set of D.*

Proof. It can be seen that the convex hull of $D \bigcup \{s_1, \cdots, s_k\}$ satisfies conditions 1) and 2) in Definition 2.2. If D is convex and $\{s_1, \cdots, s_k\} \subseteq D$, D is equal to this convex hull. By Definition 2.2, $\{s_1, \cdots, s_k\}$ is an inner convex set of D. □

Suppose that $\varepsilon_1, \cdots, \varepsilon_k$ are the standard basis vectors in $\mathbb{R}^k$. Firstly, let's set D on the s-dimensional coordinate plane, *i.e.* consider D as a subset of $\mathbb{R}^{s+k}$ with k zeros as last k components. Then after raising s_i as (s_i, ε_i), for $i = 1, \cdots, k$, a $(k+s)$-dimensional set appears with D as an s-dimensional face, $(k+s)$-dimensional points (s_i, ε_i), for $i = 1, \cdots, k$ as vertices. This $(k+s)$-dimensional set can be written as $V(D; s_1, \cdots, s_k)$.

https://doi.org/10.4208/nmtma.2016.y14020 Published online by Cambridge University Press

Definition 2.3. *(Definition for a multivariate spline with given support) With D as support and its inner convex set $\{s_1, \cdots, s_k\}$, an s-variate k-order spline, $B(x|D; s_1, \cdots, s_k)$, is the polyhedral spline given by polyhedron $V(D; s_1, \cdots, s_k)$ and linear map R_s in formula* (2.3)*. Moreover, $s_1, \cdots, s_k$ are inner points, $B(x|D; s_1, \cdots, s_k)$ is an inner point spline.*

Theorem 2.1. *If an inner point s_i is on C, an $s-1$ dimension boundary face of support D, $B(x|D; s_1, \cdots, s_k)$ is discontinuous across convex hull of this boundary face C and s_i.*

Proof. It can be seen that the $(k+s)$-dimensional points (s_i, ε_i) and the given face C form face F, a face of polyhedron $V(D; s_1, \cdots, s_k)$. With linear map R_s in formula (2.3), $R_s(F) = C$. Since $B(x|D; s_1, \cdots, s_k)$ is the polyhedral spline with polyhedron $V(D; s_1, \cdots, s_k)$ and linear map R_s, Theorem 2.1 is true by Lemma 2.1. □

Theorem 2.1 is a geometrical result. For a meaningful inner point spline, D should satisfy that:

$$vol_s(D) > 0, \quad vol_{k+s}(V(D; s_1, \cdots, s_k)) > 0.$$

In fact,

$$vol_{k+s}(V(D; s_1, \cdots, s_k)) = \frac{s!}{(k+s)!} vol_s(D).$$

By polyhedral spline in Definition 2.1, the s-variate k-order spline, $B(x|D; s_1, \cdots, s_k)$, can be expressed as

$$B(x|D; s_1, \cdots, s_k) = vol_k(V(D; s_1, \cdots, s_k) \bigcap R_s^{-1}(x)), \ x \in I\!R^s \tag{2.5}$$

Specially, if D is an s-dimensional polyhedron with points $t_1, \cdots, t_n$ as vertices we can write

$$B(x|D; s_1, \cdots, s_k) = B(x|t_1, \cdots, t_n; s_1, \cdots, s_k) \tag{2.6}$$

And to this spline, points $t_1, \cdots, t_n$ are boundary knots and $s_1, \cdots, s_k$ are inner knots. Now we call this spline *inner knot spline*.

By Lemma 2.1 for polyhedral splines, the inner knot spline in (2.6) is generally a piecewise C^{k-1}-polynomial of degree k. In additional to Theorem 2.1, we have

Theorem 2.2. *(Basic theorem for an inner knot spline) An inner knot spline function $B(x|t_1, \cdots, t_n; s_1, \cdots, s_k)$ in formula* (2.6) *is a piecewise polynomial of degree k with discontinuities only across C of dimension $s-1$ of a convex hull of some subset which is included in union of $\{s_1, \cdots, s_k\}$ and $\{t_1, \cdots, t_n\}$. To be precise, if C has dimension $s-1$ and d is the maximum dimension of a face F such that $C = R_s(F)$, then $B(x|t_1, \cdots, t_n; s_1, \cdots, s_k)$ has continuous derivatives of order $k+s-d-2$ across C.*

Proof. In fact, the set of vertices of the polyhedron for $B(x|t_1, \cdots, t_n; s_1, \cdots, s_k)$ in formula (2.6) is some subset of Q:

$$Q \equiv \{(s_i, \varepsilon_i) : i = 1, \cdots, k\} \bigcup \{(t_j, 0) : j = 1, \cdots, n\}.$$

https://doi.org/10.4208/nmtma.2016.y14020 Published online by Cambridge University Press

With linear map R_s in formula (2.3),

$$R_s(Q) = \{s_i : i = 1, \cdots, k\} \bigcup \{t_j : j = 1, \cdots, n\}.$$

And support of $B(x|t_1, \cdots, t_n; s_1, \cdots, s_k)$ is contained in the convex hull of $R_s(Q)$.

On another hand, the set of vertices of any face F for this polyhedron is some subset of Q. $C = R_s(F)$ is contained in the convex hull of the vertices of face $R_s(F)$. The vertices belong to $R_s(Q)$.

Now, Theorem 2.2 is true by Lemma 2.1. □

If $s = 1$, an inner knot spline is always defined on an interval, *i.e.* the related support is always an interval. According to Definition 2.2, this spline possesses two boundary knots. As for each of k-order splines, there are k inner knots. It can be concluded that every k-order spline possesses $(k + 2)$ knots. Since each support for all of the splines is in one form: interval, the number of boundary knots is always 2. Hence, $(k + 2)$, the number of knots, strictly depends on the order of the spline.

As for $s > 1$, it is a little different. Now a support could be any suitable polygon or polyhedron in a planar or higher dimensional space. It is easy to see that the numbers of boundary knots could be any values of positive integers.

However, whether $s = 1$ or not, it can be concluded that

Proposition 2.1. *The number of the inner knots of an s-variate k-order spline is strictly equal to its order number k. If $s = 1$, there are only two boundary knots. If $s > 1$, there are at least $s + 1$ boundary knots.*

2.3. Rational blending shape

Definition 2.4. *(Definition for a rational blending shape) A rational s-dimensional blending shape is defined as:*

$$P(t) = \sum_{i \in \mathbb{D}} B_i(t)\omega_i P_i / \sum_{i \in \mathbb{D}} \omega_i B_i(t) = \sum_{i \in \mathbb{D}} \frac{\omega_i B_i(t)}{\sum_{j \in \mathbb{D}} \omega_j B_j(t)} P_i \tag{2.7}$$

where $\mathbb{D}$ is an index set. And each $B_i(t)$, $t \in \mathbb{R}^s$ is an s-variate function related to a given control point $P_i \in \mathbb{R}^m$. $\omega_i \geq 0$ for every i and at least there is one $\omega_i > 0$.

Similarly to the NURBS curves and surfaces, $\omega_i \geq 0$ could be explained as *weight*. It is easy to see that $P(t)$ in formula (2.7) is a vector function and $B_i(t)$ are value functions. And as a function, $P(t)$ can inherit the mathematical properties of $B_i(t)$. Here are some properties.

Proposition 2.2. *(Globality) $P(t)$ in formula* (2.7) *exists all over the parametric space where $B_i(t)$ exist. And $P(t)$ is an s-dimensional geometric shape in space where the control points $\{P_i\}$ reside.*

Proposition 2.3. *(Continuity) $P(t)$ in formula* (2.7) *is C^k-continuous if each of $\{B_i(t)\}$ is C^k-continuous.*

https://doi.org/10.4208/nmtma.2016.y14020 Published online by Cambridge University Press

Since

$$\sum_{i\in\mathbb{ID}} \frac{\omega_i B_i(t)}{\sum_{j\in\mathbb{ID}} \omega_j B_j(t)} = 1, \tag{2.8}$$

we have

Proposition 2.4. *(Affine Invariance) $P(t)$ in formula* (2.7) *is affine invariance, that is, $P(t)$ is geometrically invariant under translation and rotation.*

Proposition 2.5. *(Convex Hull Property) If $B_i(t) \geq 0,\ \omega_i \geq 0$ for $i \in \mathbb{ID}$, $P(t)$ in formula* (2.7) *resides in the convex hulls of the control points $P_i, i \in \mathbb{ID}$.*

For sake of convenience, we have:

Definition 2.5. *(Definition for a rational spline shape) A rational spline shape is a $P(t)$ in formula* (2.7) *with spline functions $B_i(t), i \in \mathbb{ID}$.*

Besides Proposition 2.2-Proposition 2.5, rational spline shapes possess the other properties bellow.

Proposition 2.6. *(Locality) A rational spline shape $P(t)$ in formula* (2.7) *is generated locally.*

Proof. The reason for Proposition 2.6 is that the supports for splines are always bounded and there are only finite number of spline functions $B_i(t) > 0$ for any pre-given parameter $t \in \mathbb{R}^s$. □

With bounded supports of splines $\{B_i(t)\}$, a control point P_i affects $P(t)$ only in a bounded domain. And $P(t)$ is piecewise consists of rational spline shape components.

In addition, $\{B_i(t)\}$ can be defined in a bounded or unbounded domain, or even in disconnected domain, or a domain with holes. The terms of $P(t)$ in formula (2.7) can be any of the positive integers.

And spline $\{B_i(t)\}$ are usually non-negative, $P(t)$ resides only in the convex hulls of some parts of the related control points not in the entire convex hull of all the control points. That's $P(t)$ resides in a smaller set to the entire convex hull as stated in Proposition 2.5.

Definition 2.6. *(Definition for stable points and stable patches) Suppose that $P_k(t)$ is a surface over meshes M_k for every $k \in$ some index set $\mathbb{ID}$. If point $P_k(t_0)$ is constant for all $k \in \mathbb{ID}$, $P_k(t_0)$ is a stable point or $P_k(t)$ is stable at $t = t_0$.*

Stable patch of $P_k(t)$ is consisted of stable points of $P_k(t)$. The others are unstable points and unstable patches.

If there is only one surface over one mesh M in boundary domain, the other implicit surfaces are usually understood as surfaces over the mesh which exist in a larger domain.

Since Proposition 2.6, stable patch of rational spline shapes $P_i(t)$ usually exists.

In practical application, usually there are only a finite number of control points P_i and $P(t)$ is valid only in a bounded domain. However, $P(t)$, as a rational spline shape, can always be generated in parameter space. Actually, valid patches of $P(t)$ are exactly understood as its stable patches.

https://doi.org/10.4208/nmtma.2016.y14020 Published online by Cambridge University Press

Proposition 2.7. *(Extended easily) Along with adding or removing a control point P_i, only a certain number of pieces of rational spline shape components in $P(t)$ increases or decreases. But, $P(t)$, as a spline shape, remains.*

Example 2.1. Let index set $\mathbb{ID}$ in formula (2.7) be integer set, and

$$\Big\{B_i(t) : t \in \mathbb{R}, i \in \mathbb{ID}\Big\}$$

be the B-spline functions based on a given knot series. The rational spline shape $P(t)$ with $s = 1$ is a NURBS curve.

Example 2.2. Let index set $\mathbb{ID}$ in formula (2.7) be the set of integer pair: $\{(i, j) : i, j$ are integers$\}$, and

$$\Big\{B_{i,j}(t) = B_i(u)B_j(v) : t = (u, v) \in \mathbb{R}^2, (i, j) \in \mathbb{ID}\Big\}$$

be the products of the univariate B-spline functions $B_i(u)$ and $B_j(v)$ based on given knot series. The rational spline shape $P(t)$ with $s = 2$ is a tensor product NURBS surfaces.

Example 2.3. Let index set $\mathbb{ID}$ in formula (2.7) be the set of integer triples

$$\Big\{(i, j, k) : 0 \le i, j, k \le n; i + j + j = n\Big\},$$
$$\left\{ \begin{array}{r} B_{i,j,k}(t) = \dfrac{n!}{i!j!k!}u^i v^j w^k : 0 \le u, v, w \le 1, u + v + w = 1; \\ t = (u, v, w) \in \mathbb{R}^2, (i, j, k) \in \mathbb{ID} \end{array} \right\}$$

be triangular Bernstein functions. The rational blending shape $P(t)$ with $s = 2$ is a rational triangular Bézier surface.

2.4. Splines over a mesh in $\mathbb{R}^s$

Function family $\{B_i(t), i \in \mathbb{ID}\}$ above play a key role in designing a suitable rational blending shape $P(t)$ in formula (2.7). One of the well known examples is NURBS curves and surfaces.

The key problems related to a rational spline shape are involved in a mesh and its knots as well as some splines and related control points.

Let M be a arbitrary mesh in $\mathbb{R}^s$ for $s \ge 1$. M can be a hybrid mesh. For $s > 1$, a hybrid mesh can be a combination of triangular, quadrilateral, rectangular or any other meshes. The vertices in M are knots. For $s = 1$, the mesh is always consists of intervals.

As a family of splines, $\{B_i(t)\}$ above are usually defined over certain hybrid mesh. Therefore, control points $\{P_i\}$ which are associated with the splines should be distributed in the hybrid mesh.

First of all, let's develop a method for defining an inner knot multivariate spline in any pre-given mesh M in $\mathbb{R}^s$.

https://doi.org/10.4208/nmtma.2016.y14020 Published online by Cambridge University Press

Definition 2.7. *(Definition for support of a knot set in mesh M) Let $s_1, \cdots, s_k$ be knots in M. $supp\{s_1, \cdots, s_k\}$ is the smallest polyhedron which satisfies:*
1) *There are knots $\{t_1, \cdots, t_n\}$ in M, such that*

$$supp\{s_1, \cdots, s_k\} = [t_1, \cdots, t_n];$$

2) $\{t_1, \cdots, t_n\} \bigcap \{s_1, \cdots, s_k\}$ *is empty;*
3) $[s_1, \cdots, s_k] \subseteq supp\{s_1, \cdots, s_k\}$ *;*
4) *For $j = 1, \cdots, n$, t_j are on the boundary of $supp\{s_1, \cdots, s_k\}$.*

Theorem 2.3. *For knots $s_1, \cdots, s_k$ in mesh M, if there is at least one set which satisfies the 4 conditions in Definition* 2.7*, $supp\{s_1, \cdots, s_k\}$ exists.*

Proof. The reason is that intersection of any two sets which satisfy the 4 conditions satisfies the 4 conditions, too. □

Corollary 2.1. *Suppose that a knot set $T_0 = T_0(s_1, \cdots, s_k)$ is*

$$T_0 = \{t : t \text{ is a knot from } M, \text{ and for some } s_i, \ \overline{ts_i} \text{ is an edge of } M\},$$

and $\{s_1, \cdots, s_k\}$ is contained in $[T_0]$, the convex hull of T_0, then support $supp\{s_1, \cdots, s_k\}$ exists.

Proof. Since $\{s_1, \cdots, s_k\}$ is contained in the convex hull of T_0, $[s_1, \cdots, s_k]$ is contained in the convex hull of T_0. Moreover, $supp\{s_1, \cdots, s_k\}$ exists based on Theorem 2.3. □

If $\{s_1, \cdots, s_k\}$ is given, knot set $T_0(s_1, \cdots, s_k)$ can be constructed intutively. Therefore, Corollary 2.1 can be used to construct $supp\{s_1, \cdots, s_k\}$.

Let knot set $T_M = T_M(s_1, \cdots, s_k)$ be

$$T_M = \Big\{t : t \text{ is a knot from } M, \text{ but } t \text{ is not a inner point of } [s_1, \cdots, s_k].\Big\}.$$

Proposition 2.8. *For any knot set $\{s_1, \cdots, s_k\}$ in mesh M, $T_0 = T_0(s_1, \cdots, s_k)$ is always a subset of $T_M = T_M(s_1, \cdots, s_k)$.*

Proposition 2.9. *For any knot sets $\{s_1, \cdots, s_k\}$ and $\{t_1, \cdots, t_n\}$ in mesh M, if $[s_1, \cdots, s_k] \subseteq [t_1, \cdots, t_n]$, $[t_1, \cdots, t_n] \subseteq [T_M] = [T_M(s_1, \cdots, s_k)]$.*

Proof. Any knot set $T = \{t_1, \cdots, t_n\}$ can be divided into two subsets:

$$T_1 = \Big\{t \in T, \text{ but } t \text{ is not a inner point of } [s_1, \cdots, s_k].\Big\},$$

$$T_2 = T - T_1 = \Big\{t \in T, \text{ but } t \text{ is a inner point of } [s_1, \cdots, s_k].\Big\} \subset [s_1, \cdots, s_k].$$

If $[s_1, \cdots, s_k] \subseteq [t_1, \cdots, t_n]$, each point of T_2 is a inner point of $[t_1, \cdots, t_n]$. This fact implies $[T_1] = [t_1, \cdots, t_n]$. By the definition of T_M, $T_1 \subseteq T_M$. Now, $[t_1, \cdots, t_n] = [T_1] \subseteq [T_M]$. □

If Condition 1) in Definition 2.7 holds, it is easy to see that $[t_1, \cdots, t_n] \subseteq T_0(s_1, \cdots, s_k)$. Associated with Theorem 2.3, Theorem 2.4 holds.

https://doi.org/10.4208/nmtma.2016.y14020 Published online by Cambridge University Press

Theorem 2.4. *For knots $s_1, \cdots, s_k$ in mesh M, $supp\{s_1, \cdots, s_k\}$ exists if and only if $[s_1, \cdots, s_k] \subseteq [T_M]$.*

Proof. If $[s_1, \cdots, s_k] \subseteq [T_M]$, Theorem 2.4 holds from Theorem 2.3. On other hands, if $supp\{s_1, \cdots, s_k\}$ exists, then there is knot set $T = \{t_1, \cdots, t_n\}$, such that $supp\{s_1, \cdots, s_k\} = [T]$, and $[s_1, \cdots, s_k] \subseteq supp\{s_1, \cdots, s_k\} = [T]$. By Proposition 2.9, $[s_1, \cdots, s_k] \subseteq [T] \subseteq [T_M]$. □

Definition 2.8. *(Definition for an inner knot multivariate spline in mesh M) Let $s_1, \cdots, s_k$ be knots in M in $\mathbb{R}^s$, and $supp\{s_1, \cdots, s_k\} = [t_1, \cdots, t_n]$ exists. Then, by Definition 2.3, an s-variate k-order spline $B(x|t_1, \cdots, t_n; s_1, \cdots, s_k)$ may follow. Denote this spline by*

$$B_M(t|t_1, \cdots, t_n; s_1, \cdots, s_k), \tag{2.9}$$

as a spline of $\{s_1, \cdots, s_k\}$ in M.

If necessary, $supp\{s_1, \cdots, s_k\}$, as a convex set, can be modified , such that $\{s_1, \cdots, s_k\}$ is an inner convex set by Definition 2.2. In this way, mesh spline can be defined by non convex support or other reasonable polyhedrons. In Example 3.1 in the next section, $supp\{s_1, \cdots, s_k\}$ is modified so that a support consists of polygons from the given mesh. However, $supp\{s_1, \cdots, s_k\}$ can be a choice of various sets. For existence of spline $B(x|t_1, \cdots, t_n; s_1, \cdots, s_k)$, $supp\{s_1, \cdots, s_k\}$ should be an inner convex set.

If there is a proper number of this kind of s-variate k-order splines in M, with related control points, a rational s-variate k-order spline shape defined by Definition 2.5 above appears.

Example 2.4. Let $s = 1$, and M is a non-decreasing knot series $\{s_i : -\infty < i < \infty\}$. For any integer i, there are k adjacent knots $s_{i+1}, s_{i+2}, \cdots, s_{i+k}$. Take $t_1 = s_i$ and $t_2 = s_{i+k+1}$. Knot interval $[t_1, t_2] = [s_i, s_{i+k+1}]$ is the smallest knot interval which contains knots $s_{i+1}, s_{i+2}, \cdots, s_{i+k}$.

Then by formula (2.9), we have a spline

$$B_{i,k}(t) = B_M(t|s_i, s_{i+k+1}; s_{i+1}, \cdots, s_{i+k}).$$

$B_{i,k}(t)$ is an univariate k-order B-spline with knots $s_{i+k}, s_{i+k+1}, \cdots, s_{i+k+1}$. And as the number of boundary knots, n in Definition 2.8 is always 2.

With those B-splines $B_{i,k}(t)$, NURBS curves have been constructed.

For $s = 2$, bivariate splines and the rational spline shape on mesh M can still be constructed. And n, as the number of boundary knots, can be any positive integer. Of course, n depends on the given mesh M. Based on Theorem 2.1, n varies in the given mesh M. And k, as the number of inner knots, is always equal to the order number of the related spline. k is independent of the given mesh.

Box splines and simplex splines have been used to develop spline surfaces over certain meshes in a similar way, [11]. In the sections below, the key aim is to develop families of inner knot splines in reasonable ways. For $k = 1, 2, 3$, $\{B_i(t)\}$, as well as the related $\{P_i\}$, are designed based on various given hybrid meshes, then follow C^{k-1}-continuous surfaces reasonably.

https://doi.org/10.4208/nmtma.2016.y14020 Published online by Cambridge University Press

3. C^0- and C^1-surfaces over hybrid meshes

3.1. Bivariate linear splines and C^0-surfaces over hybrid meshes

Suppose that $I\!D$ is an index set, $\{s_i, i \in I\!D\}$ is the knot set of a given mesh M defined in Subsection 2.4.

For every s_i, denote a knot set by

$$T_i = \{t_{i,j} : \text{ there is an edge between } t_{i,j} \text{ and } s_i\}.$$

Proposition 3.1. *If s_i is in the convex hull of T_i, this convex hull can be chosen as $supp\{s_i\}$.*

Now with s_i as inner knot and its $supp\{s_i\}$, a linear spline is generated based on Definition 2.8 and equation (2.6). Denote it by $B_{i,M}(t|s_i)$ or $B_{i,M}(t)$. The related control point P_i to $B_{i,M}(t|t_j,\ j = 1, \cdots, n)$ can also be considered as a point residing at the given knot s_i.

With $\{B_{i,M}(t), i \in I\!D\}$, a family of linear splines over M, a linear rational spline shape $P(t)$ is generated by formula (2.7). For $s = 1$, $P(t)$ is a linear NURBS curve.

For $s = 2$, $P(t)$ is a C^0-surface consisting of piecewise planar polygons.

Proposition 3.2. *Piecewise planar polygons over hybrid meshes are rational C^0 spline surfaces.*

There are more details about this $P(t)$ in [10].

3.2. Bivariate quadratic splines and C^1-surfaces over hybrid meshes

Suppose that $I\!D$ is an index set, $\{E_i, i \in I\!D\}$ is the edge set of a given mesh M. For every edge E_i, there always are two knots s_{i0} and s_{i1} as its ends. Denote a knot set by

$$T_i = \Big\{t_{i,j} : \text{ there is an edge between } t_{i,j} \text{ and one of } s_{i0}, s_{i1}\Big\}.$$

Proposition 3.3. *If edge $E_i = \overline{s_{i0}s_{i1}}$ is in the convex hull of T_i, this convex hull can be chosen as $supp\{s_{i0}, s_{i1}\}$.*

Now with s_{i0} and s_{i1} as inner knots, and their $supp\{s_{i0}, s_{i1}\}$, a quadratic spline, is generated based on Definition 2.8 and Eq. (2.6). Denote it by $B_{i,M}(t|s_{i0}, s_{i1})$ or $B_{i,M}(t)$. The related control point P_i to $B_{i,M}(t)$ can also be considered as a point residing on edge $E_i = \overline{s_{i0}s_{i1}}$.

With $\{B_{i,M}(t), i \in I\!D\}$, a family of quadratic splines over M, a quadratic rational spline shape $P(t)$ is generated by formula (2.7). For $s = 1$, $P(t)$ is a quadratic NURBS curve.

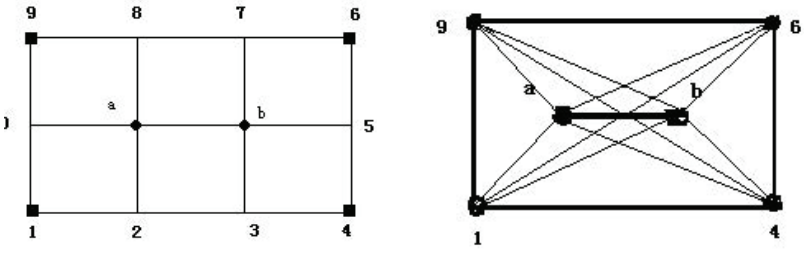
For $s = 2$, parameter $t = (u, v) \in I\!R^2$, $B_{i,M}(t) = B_{i,M}(u, v)$, $P(t) = P(u, v)$ is usually a C^1-surface consisting of piecewise bivariate polynomials of degree 2. Here is an example.

https://doi.org/10.4208/nmtma.2016.y14020 Published online by Cambridge University Press

Example 3.1. (Bivariate quadratic splines over a rectangular mesh M) Suppose M is a rectangular mesh. As shown in Fig. 1(a), edge $\overline{ab}$ has two end-knots: a and b. For edge $\overline{ab}$, define knot set

$$T_{ab} = \{t : \text{ there is an edge between } t \text{ and one of } a, b \} = \{0, 2, 3, 5, 7, 8\}.$$

Convex hull of T_{ab} which contains edge $\overline{ab}$ is a union of rectangles and triangles. As a rectangular mesh, M is just a union of rectangles, T_{ab} is extended as $T_{ab} = \{0, 1, 2, 3, 4, 5, 6, 7, 8, 9\}$. Now, convex hull of extended T_{ab}, *i.e.*, $supp\{a, b\}$ is a rectangle consisting of 6 smaller rectangles in the given rectangular mesh M. Based on Definition 2.8 and Eq. (2.6), a bivariate quadratic spline for edge $\overline{ab}$: $B_M(u, v|0, 1, 2, 3, 4, 5, 6, 7, 8, 9; a, b)$ is generated.



(a) (b)

Figure 1: Support for bivariate quadratic spline on rectangular mesh.

The 2 inner knots are a and b; the 10 boundary knots are $1, 2, 3, 4, 5, 6, 7, 8, 9$ and 0. Geometrically, six knots $2,\ 3,\ 5,\ 7,\ 8$ and 0 can be neglected as they are respectively on edges $\overline{14},\ \overline{46},\ \overline{69}$ and $\overline{91}$. Hence, this spline can be written as $B_M(u, v|1, 4, 6, 9; a, b)$.

$B_M(u, v|1, 4, 6, 9; a, b)$ is a piecewise polynomial of degree 2. Its support includes 17 edges related to 17 splines. The number of the pieces of polynomials is equal to 18, the number of the subsets in the support for this bivariate quadratic spline, as shown in Fig. 1(b).

The polyhedron for $B_M(u, v|1, 4, 6, 9; a, b)$ can be divided into two 4-dimensional and zero-volume-intersection simplexes: $146ab$ and $169ab$. Actually, these two simplexes share a 3 dimensional face given by $16ab$. And they lie in opposite sides of face $16ab$. There is a scheme for numerical computation of splines on simplex in [11].

By Lemma 2.1, we have

Theorem 3.1. *$B_M(u, v|1, 4, 6, 9; a, b)$ is a C^1-piecewise quadratic polynomial.*

$B_M(u, v|\cdot; a, 8)$ can be obtained by rotating $B_M(u, v|1, 4, 6, 9; a, b)$ around point a such that point b meets point 8. The other splines in M can be obtained by translating either of those two splines.

$B_M(u, v|1, 4, 6, 9; a, b)$ and $B_M(u, v|\cdot; a, 8)$ are computed in [12].

Suppose that knots have integer coordinates. As shown in Fig. 1(a), if coordinates of knots a, b and 8 are (i, j), $(i + 1, j)$ and $(i, j + 1)$, edges $\overline{ab}$ and $\overline{a8}$ can be indexed by

https://doi.org/10.4208/nmtma.2016.y14020 Published online by Cambridge University Press

$(i,j,0)$ and $(i,j,1)$, respectively. With those indexes, edges in rectangular mesh M can be indexed by index set

$$\mathbb{D} = \Big\{(i,j,k) : i,j = 0,\pm1,\pm2,\cdots;k = 0,1\Big\}. \tag{3.1}$$

And $B_M(u,v|1,4,6,9;a,b)$ as well as $B_M(u,v|\cdot;a,8)$, can be denoted as $B_{i,j,0}(u,v)$ and $B_{i,j,1}(u,v)$, respectively.

Theorem 3.2. *With a family of splines $\{B_{i,j,k}(u,v) : (i,j,k) \in \mathbb{D}\}$, and control points $\{P_{i,j,k} : (i,j,k) \in \mathbb{D}\}$, weights $\{\omega_{i,j,k} : (i,j,k) \in \mathbb{D}\}$, the rational C^1-spline surface $P(u,v)$ by* (2.7) *over rectangular mesh M is expressed as:*

$$P(u,v) = \frac{\sum\limits_{i=-\infty}^{\infty}\sum\limits_{j=-\infty}^{\infty}\sum\limits_{k=0}^{1}\omega_{i,j,k}B_{i,j,k}(u,v)P_{i,j,k}}{\sum\limits_{i=-\infty}^{\infty}\sum\limits_{j=-\infty}^{\infty}\sum\limits_{k=0}^{1}\omega_{i,j,k}B_{i,j,k}(u,v)}, \quad t=(u,v)\in\mathbb{R}^2, \tag{3.2}$$

For this $P(u,v)$, more details about the boundary property, the corner property, the derivative property and smooth connecting conditions of different patches are presented in sections from 6 to 10.

4. A heart-repairing technique

It can be deduced by Lemma 2.1 or Theorem 2.2 that $B_M(t|1,4,6,9;a,b)$ can be discontinuities if the inner knots and the boundary knots are colinear. But, in some regular meshes used usually all of knots are distributed on lines in certain few given directions, such as triangular Bézier type meshes or rectangular meshes in only 3 or 2 given directions. Therefore, the colinear knots in meshes are almost indispensable and unexpected discontinuities of multivariate splines may appear.

By Lemma 2.1, the original bivariate quadratic splines in triangular Bézier type meshes are just continuous [13]. However, by adjusting inner knots, C^1-splines and related C^1-surfaces are possible.

Proposition 4.1. *(Heart-Repairing Technique) By only adjust inner knots, the unexpected discontinuities of splines are avoided. And so is that of the related rational spline surface or spline shape in general. Meanwhile, boundary knots as well as the supports of the splines still remain. And so are the mesh structures and the related control points.*

This method is a spline heart-repairing technique for higher order of smoothness, without changing the other properties.

This *heart-repairing technique* seems usually indispensable for multivariate splines with given supports in specific meshes to avoid unexpected discontinuities. This is true in examples in the following sections.

https://doi.org/10.4208/nmtma.2016.y14020 Published online by Cambridge University Press

However, the original bivariate quadratic splines and the related surface in a uniform rectangular mesh in Example 3.1 are C^1-continuous. That is the heart-repairing technique is not necessary for rectangular mesh spline surfaces.

C^0- and C^1-surfaces over hybrid mesh above are spline surfaces, different from that of spline tensor product surfaces. The surfaces above are in form of piecewise polynomials with degree respectively one or two, comparing to that of 1×1, 2×2 spline tensor product surfaces with degree respectively two or four.

5. C^2-surfaces over triangular meshes

Suppose that $\mathbb{ID}$ is an index set, $\{\triangle_i, i \in \mathbb{ID}\}$ is the triangle set of a triangular mesh M. A triangle $\triangle_i, i \in \mathbb{ID}$ should be usually understood as the smallest triangle which includes no other triangles in M. With a triangle $\triangle_i, i \in \mathbb{ID}$, there always are three knots s_{i0} , s_{i1} and s_{i2} as its three vertices. Denote a knot set by

$$T_i = \Big\{ t_{i,j} : \text{ there is an edge between } t_{i,j} \text{ and one of } s_{i0},\ s_{i1} \text{ or } s_{i2} \Big\}.$$

Proposition 5.1. *If triangle $\triangle_i = \triangle(s_{i0}, s_{i1}, s_{i2})$ is in the convex hull of T_i, this convex hull can be chosen as $supp\{s_{i0}, s_{i1}, s_{i2}\}$.*

Now with s_{i0}, s_{i1} and s_{i2} as inner knots and their $supp\{s_{i0}, s_{i1}, s_{i2}\}$, a cubic spline is generated based on Definition 2.8 and Eq. (2.6), which will be denoted by $B_{i,M}(t|s_{i0}, s_{i1}, s_{i2})$ or $B_{i,M}(t)$.

The related control point P_i to $B_{i,M}(t)$ can also be considered as a point residing over triangle $\triangle_i$.

With $\{B_{i,M}(t), i \in \mathbb{ID}\}$, a family of splines over M, a rational cubic spline shape $P(t)$, is generated by (2.7). For $s = 1$, a triangle can be understood as three consecutive knots in a knot series. And this $P(t)$ is a cubic NURBS curve.

For $s = 2$, parameter $t = (u, v) \in \mathbb{R}^2$ and $B_{i,M}(t) = B_{i,M}(u, v)$, $P(t) = P(u, v)$ is usually a C^2-surface consisting of piecewise bivariate polynomials with degree 3. An example is stated below.

Example 5.1. (Bivariate cubic splines over a triangular Bézier type mesh) As shown in Fig. 2(a), if M is a mesh similar to that of a triangular Bézier surface, $\triangle abc$, one of the smallest triangle in M, has three vertex knots: a, b, c.

Let knot set

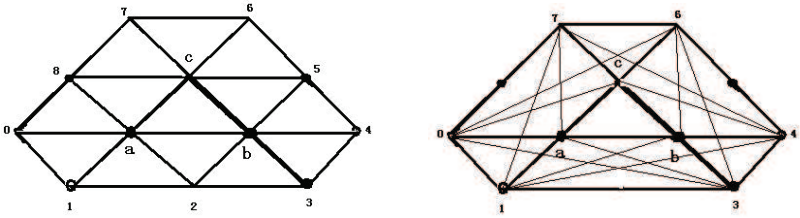
$$\begin{aligned} T_{abc} &= \{t : \text{ there is an edge between } t \text{ and one of } a, b, c \ \} \\ &= \{0, 1, 2, 3, 4, 5, 6, 7, 8\}. \end{aligned}$$

Convex hull of T_{abc} which includes knots a, b and c, is a union of triangles in M, and can be used as support $supp\{a, b, c\}$. Based on Definition 2.8 and Eq. (2.6), there is a bivariate cubic spline for triangle $\triangle abc$ in M:

$$B_M(u, v|0, 1, 2, 3, 4, 5, 6, 7, 8; a, b, c).$$

https://doi.org/10.4208/nmtma.2016.y14020 Published online by Cambridge University Press

For this spline with $\triangle abc$, the 3 inner knots are a, b and c; the 9 boundary knots are $0, 1, 2, 3, 4, 5, 6, 7$ and 8. Geometrically, knots $2, 5$ and 8 can be neglected as they are on edges $\overline{13}$, $\overline{46}$ and $\overline{70}$, respectively. Hence, this spline can be written as $B_M(u, v|0, 1, 3, 4, 6, 7; a, b, c)$.



(a) (b)

Figure 2: Support for bivariate cubic spline on triangular Bézier type mesh.

$B_M(u, v|0, 1, 3, 4, 6, 7; a, b, c)$ is a piecewise polynomial of degree 3. Its support includes 13 triangles related to 13 splines. As shown in Fig. 2(b), the number of the pieces of polynomials is equal to 41, the number of the subsets in the support for this bivariate cubic spline.

The 5-dimensional polyhedron for $B_M(u, v|0, 1, 3, 4, 6, 7; a, b, c)$ can be divided into four 5-dimensional and zero-volume-intersection simplexes: $013abc$, $034abc$, $046abc$ and $067abc$. Actually, 3 pairs of every two adjacent simplexes share 4 dimensional faces given by $03abc$, $04abc$ and $06abc$, respectively. And all pairs lie in opposite sides of their common faces.

Theorem 5.1. *$B_M(u, v|0, 1, 3, 4, 6, 7; a, b, c)$ can be modified as a C^2-piecewise polynomial of degree 3 without any change of its support.*

Proof. By Theorem 2.2, $B_M(u, v|0, 1, 3, 4, 6, 7; a, b, c)$ have discontinuities across lines $\overline{04}$, $\overline{16}$ and $\overline{37}$, as that edges $\overline{ab}$, $\overline{bc}$ and $\overline{ca}$ are on those three lines respectively. To avoid unexpected discontinuities across the three lines, let us apply the heart-repairing technique in Proposition 4.1 by the following scheme: adjusting the three inner knots a, b and c by zooming around their center, so that none of the changed knots a, b and c is on any of the lines $\overline{04}$, $\overline{16}$ and $\overline{37}$.

After this scheme, the new $B_M(u, v|0, 1, 3, 4, 6, 7; a, b, c)$ is a C^2-piecewise polynomial of degree 3 without any change of its support. □

As shown in Fig. 2(a), let's consider line $\overline{04}$ as an axis of symmetry. Then for knots 6 and 7, there are symmetrical knots $6'$ and $7'$, and the bivariate cubic spline for another triangle $\triangle 2ab$ in M is $B_M(u, v|0, 8, 5, 4, 6', 7'; 2, a, b)$ which is axis-symmetric with $B_M(u, v|0, 1, 3, 4, 6, 7; a, b, c)$.

Corollary 5.1. *Spline $B_M(u, v|0, 8, 5, 4, 6', 7'; 2, a, b)$ is axis-symmetric with spline $B_M(u, v|0, 1, 3, 4, 6, 7; a, b, c)$.*

The other splines in M can be obtained by translating either of two splines $B_M(u, v|0, 8, 5, 4, 6', 7'; 2, a, b)$ or $B_M(u, v|0, 1, 3, 4, 6, 7; a, b, c)$.

https://doi.org/10.4208/nmtma.2016.y14020 Published online by Cambridge University Press

Proof. Corollary 5.1 is direct by the geometrical explanation of the splines. □

Suppose that vectors $\overrightarrow{ab} = (1, 0)$ and $\overrightarrow{ac} = (1/2, \sqrt{3}/2)$, knots in a triangular Bézier type mesh can be indexed as:

$$\left\{ t_{i,j} = (u_{i,j}, v_{i,j}) = i\overrightarrow{ab} + j\overrightarrow{ac} = i(1, 0) + j(1/2, \sqrt{3}/2) : i, j = 0, \pm 1, \pm 2, \cdots \right\}.$$

As shown in Fig. 2(a), if indexes of knots a, b, c and 8 are (i, j), $(i + 1, j)$, $(i, j + 1)$ and $(i-1, j+1)$, triangle $\triangle abc$ and $\triangle ac8$ can be indexed by $(i, j, 0)$ and $(i, j, 1)$, respectively.

With those indexes, triangles in triangular Bézier type mesh M can be indexed by index set $\mathbb{ID} = \{(i, j, k) : i, j = 0, \pm 1, \pm 2, \cdots ; k = 0, 1\}$. And splines $B_M(t|1, 4, 6, 9; a, b)$, as well as $B_M(t|\cdot; a, 8)$, are denoted as $B_{i,j,0}(u, v)$ and $B_{i,j,1}(u, v)$, respectively. Another spline $B_M(u, v|0, 8, 5, 4, 6', 7'; 2, a, b)$ is indexed as $B_{i+1,j-1,1}(u, v)$.

Based on those indexes, Corollary 5.1 can be exactly expressed as

Theorem 5.2. *$B_{i,j,k}(u, v)$ are bivariate cubic C^2 splines over triangular Bézier type mesh M, satisfying*

1)
$$B_{i,0,0}(u, v) = B_{i,-1,1}(u, -v);$$

2)
$$B_{i,j,k}(u, v) = B_{0,0,k}(u - i - j/2, v - j\sqrt{3}/2).$$

With those splines $\{B_{i,j,k}(u, v)\}$ over triangular Bézier type mesh M, we have

Theorem 5.3. *The related $P(u, v)$ by* (2.7) *is a rational cubic C^2-surface over triangular Bézier type mesh M.*

6. Rational bivariate quadratic C^1-surfaces over rectangular mesh

In Example 3.1 in Section 3, bivariate C^1-quadratic splines over a rectangular mesh M are discussed. For an index $(i, j, k) \in \mathbb{ID}$(defined in formula (3.1)), the related spline and control point can be written as $B_{i,j,k}(u, v)$ and $P_{i,j,k}$, respectively. From the Example 3.1, $B_{i,j,k}(u, v)$ is a piecewise quadratic C^1-polynomials function.

Geometrically, $B_{i,j,0}(u, v)$ satisfies Lemma 6.1, Lemma 6.2 and Lemma 6.3.

Lemma 6.1. *For $(i, j, k) \in \mathbb{ID}$,*

$$B_{i,j,k}(u + m, v + n) = B_{i-m,j-n,k}(u, v). \tag{6.1}$$

Proof. As mentioned in Example 3.1 in Section 3, if the polyhedron for $B_{i,j,k}(u, v)$ is moved from point (i, j) to $(i - m, j - n)$, it will coincide with the polyhedron for $B_{i-m,j-k,k}(u, v)$. So do $B_{i,j,k}(u, v)$ and $B_{i-m,j-k,k}(u, v)$. And the conclusion follows. □

Lemma 6.2. *For $i, j = 0, \pm 1, \pm 2, \cdots$,*

$$B_{i,j,1}(u, v) = B_{j,i,0}(v, u). \tag{6.2}$$

https://doi.org/10.4208/nmtma.2016.y14020 Published online by Cambridge University Press

Proof. It's easy to see that the polyhedrons for $B_{0,0,1}(u,v)$ and $B_{0,0,0}(v,u)$ are symmetrical about line $u-v=0$. So are $B_{0,0,1}(u,v)$ and $B_{0,0,0}(v,u)$. Associated with Lemma 6.1, Lemma 6.2 holds. □

Lemma 6.3. *The support of* $B_{i,j,0}(u,v)$ *is*

$$supp_{i,j,0}=\{(u,v): i-1\le u\le i+2; j-1\le v\le j+1\},$$

and that the support of $B_{i,j,1}(u,v)$ *is*

$$supp_{i,j,1}=\{(u,v): i-1\le u\le i+1; j-1\le v\le j+2\}.$$

Proof. The supports of $B_{i,j,k}(u,v)$ are orthogonal projections of their polyhedrons. The mathematical details are omitted. □

Corollary 6.1. *For rectangle area* $\{(u,v): m\le u\le m+1; n\le v\le n+1\}\equiv[m,m+1]\times[n,n+1]$*, the support of* $B_{i,j,0}(u,v)$ *satisfies*

$$supp_{i,j,0}\supseteq[m,m+1]\times[n,n+1]$$

if and only if

$$i=m-1,\ m,\ m+1, j=n,\ n+1.$$

Moreover, the support of $B_{i,j,1}(u,v)$ *satisfies*

$$supp_{i,j,1}\supseteq[m,m+1]\times[n,n+1]$$

if and only if

$$i=m,\ m+1, j=n-1,\ n,\ n+1.$$

Proof. Corollary 6.1 can be derived from Lemma 6.3. □

For each of pairs (m,n), denoted by

$$\begin{aligned}\mathbb{D}_{m,n}=&\{(i,j,0), i=m-1,m,m+1; j=n,n+1\}\\ &\bigcup\{(i,j,1), i=m,m+1; j=n-1,n,n+1\},\end{aligned}\tag{6.3}$$

an index set with 12 elements. $\mathbb{D}_{m,n}$ satisfies

Lemma 6.4. *For* $k=0,1$, $(i+m,j+n,k)\in\mathbb{D}_{m,n}$ *is equivalent to* $(i,j,k)\in\mathbb{D}_{0,0}$.

Based on formula (2.7), a rational bivariate quadratic C^1-surfaces over rectangular M can be constructed in formula (3.2), or, rewritten as

$$P(u,v)=\frac{\sum\limits_{(i,j,k)\in\mathbb{D}}\omega_{i,j,k}B_{i,j,k}(u,v)P_{i,j,k}}{\sum\limits_{(i,j,k)\in\mathbb{D}}\omega_{i,j,k}B_{i,j,k}(u,v)},\quad (u,v)\in\mathbb{R}^2,\tag{6.4}$$

where nonnegative constants $\omega_{i,j,k}$ are weights. Certainly, $P(u,v)$ in formula (6.4) satisfies Proposition 2.1-Proposition 2.6. Here are additional properties.

https://doi.org/10.4208/nmtma.2016.y14020 Published online by Cambridge University Press

Theorem 6.1. *$P(u,v)$ in formula* (3.2) *or formula* (6.4)*, a rational bivariate quadratic C^1-surfaces over a rectangular mesh can be locally expressed in formula* (6.5)*, as patches $P_{m,n}(u,v)$:*

$$P_{m,n}(u,v)=\frac{\sum\limits_{(i,j,k)\in\mathbb{D}_{0,0}}\omega_{i+m,j+n,k}M_{i,j,k}(u,v)P_{i+m,j+n,k}}{\sum\limits_{(i,j,k)\in\mathbb{D}_{0,0}}\omega_{i+m,j+n,k}M_{i,j,k}(u,v)},\quad (u,v)\in[0,1]\times[0,1], \tag{6.5}$$

where $M_{i,j,k}(u,v)$ for $(i,j,k)\in\mathbb{D}_{0,0}$ are C^1-quadratic splines, given by

$$M_{i,j,k}(u,v)\equiv B_{0,0,k}(u+i,v+j),(u,v)\in[0,1]\times[0,1]. \tag{6.6}$$

Proof. Based on Lemma 6.3, Lemma 6.4 and Corollary 6.1, $P(u,v)$ in formula (6.4) can be piecewise expressed as

$$P(u,v)=\frac{\sum\limits_{(i,j,k)\in\mathbb{D}_{m,n}}\omega_{i,j,k}B_{i,j,k}(u,v)P_{i,j,k}}{\sum\limits_{(i,j,k)\in\mathbb{D}_{m,n}}\omega_{i,j,k}B_{i,j,k}(u,v)},\quad (u,v)\in[m,m+1]\times[n,n+1]. \tag{6.7}$$

Replacing u with $u+m$, v with $v+n$, and $P(u+m,v+n)$ with $P_{m,n}(u,v)$, the patch $P(u,v)$ in (6.7) is:

$$P_{m,n}(u,v)=\frac{\sum\limits_{(i,j,k)\in\mathbb{D}_{m,n}}\omega_{i,j,k}B_{i,j,k}(u+m,v+n)P_{i,j,k}}{\sum\limits_{(i,j,k)\in\mathbb{D}_{m,n}}\omega_{i,j,k}B_{i,j,k}(u+m,v+n)},\quad (u,v)\in[0,1]\times[0,1]. \tag{6.8}$$

Evidently, $P_{m,n}(u,v),(u,v)\in[0,1]\times[0,1]$ is a patch of surface $P(u,v),(u,v)\in\mathbb{R}^2$. And surface $P(u,v),(u,v)\in\mathbb{R}^2$ is composed of all of its patches.

Associated with Lemma 6.1, $P_{m,n}(u,v)$ can be expressed as

$$P_{m,n}(u,v)=\frac{\sum\limits_{(i,j,k)\in\mathbb{D}_{0,0}}\omega_{i+m,j+n,k}B_{i,j,k}(u,v)P_{i+m,j+n,k}}{\sum\limits_{(i,j,k)\in\mathbb{D}_{0,0}}\omega_{i+m,j+n,k}B_{i,j,k}(u,v)},\quad (u,v)\in[0,1]\times[0,1], \tag{6.9}$$

or

$$P_{m,n}(u,v)=\frac{\sum\limits_{(i,j,k)\in\mathbb{D}_{0,0}}\omega_{i+m,j+n,k}B_{0,0,k}(u+i,v+j)P_{i+m,j+n,k}}{\sum\limits_{(i,j,k)\in\mathbb{D}_{0,0}}\omega_{i+m,j+n,k}B_{0,0,k}(u+i,v+j)},\quad (u,v)\in[0,1]\times[0,1]. \tag{6.10}$$

From Eq. (6.10), surface $P(u,v)$ can be expressed by only two spline functions $B_{0,0,0}(u,v)$ and $B_{0,0,1}(u,v)$.

https://doi.org/10.4208/nmtma.2016.y14020 Published online by Cambridge University Press

As mentioned in Eq. (6.6), define $M_{i,j,k}(u,v) \equiv B_{0,0,k}(u+i, v+j)$ for $(i,j,k) \in \mathbb{ID}_{0,0}$ which are quadratic polynomials restricted in $[0,1] \times [0,1]$. $P_{m,n}(u,v)$ in Eq. (6.10) is conveniently expressed as Eq. (6.5). □

By the way, let $Q_{m',n'}(u,v)$ be a patch similar to $P_{m,n}(u,v)$, and the related control points and weights are $Q_{i,j,k}$ and $w_{i,j,k}$. Based on Eq. (6.5), $Q_{m',n'}(u,v)$ is $P_{m,n}(u,v)$ or $Q_{m',n'}(u,v) = P_{m,n}(u,v)$ which means exactly that $P_{m,n}(u,v)$ is a patch with its control points and weights satisfying

$$\omega_{i+m,j+n,k} = w_{i+m',j+n',k}, P_{i+m,j+n,k} = Q_{i+m',j+n',k}, \quad \text{for } (i,j,k) \in \mathbb{ID}_{0,0}. \tag{6.11}$$

7. Bivariate quadratic C^1-splines over rectangular mesh

For edge with index $(1,0,0)$, there are two knots $(1,0)$ and $(2,0)$ as shown in Fig. 3. As mentioned in Example 3.1 in Section 3, the polyhedron for $B_M(x|1,4,6,9;a,b) = B_{1,0,0}(u,v)$ can be divided into two 4-dimensional and zero-volume-intersection simplexes: $146ab$, $169ab$, there. Actually, these two simplexes share a 3 dimensional face given by $16ab$. And they lie in opposite sides of face $16ab$. A detailed numerical computational scheme and examples for simplex splines can be found in [11].

As a sum of two simplex splines function, $B_{1,0,0}(u,v)$ is as follows [12]:

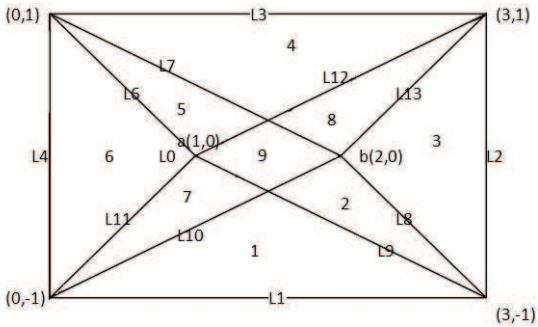


Figure 3: Support of spline $B_{1,0,0}(u,v)$.

Lemma 7.1. *Spline $B_{1,0,0}(u,v)$ is*

$$B_{1,0,0}(u,v) = \begin{cases} 2(1+v)^2, & (u,v) \in D_1 \\ 1+2u+8v-u^2-4uv-2v^2, & (u,v) \in D_2 \\ (-3+u)^2, & (u,v) \in D_3 \\ 2(-1+v)^2, & (u,v) \in D_4 \\ -2+4u+4v-u^2-4uv-2v^2, & (u,v) \in D_5 \\ u^2, & (u,v) \in D_6 \\ -2+4u-4v-u^2+4uv-2v^2, & (u,v) \in D_7 \\ 1+2u-8v-u^2+4uv-2v^2, & (u,v) \in D_8 \\ -3+6u-2u^2-6v^2, & (u,v) \in D_9 \\ 0, & \textit{otherwise} \end{cases} \tag{7.1}$$

https://doi.org/10.4208/nmtma.2016.y14020 Published online by Cambridge University Press

where D_i is shown in Fig. 3. As shown in Fig. 4, it can be verified that $B_{1,0,0}(u,v)$ is a C^1-piecewise quadratic polynomial with support $[0,3]\times[-1,1]$.

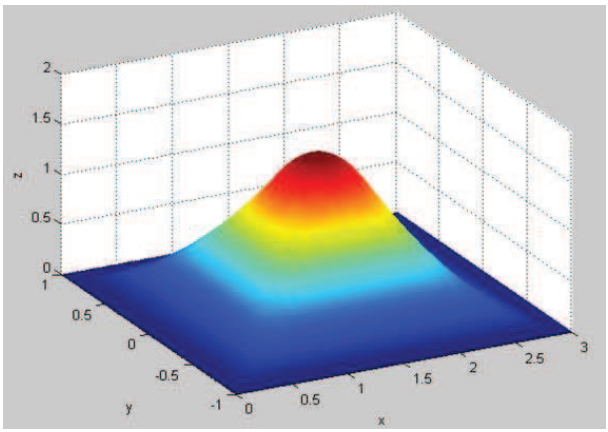


Figure 4: Image of spline $B_{1,0,0}(u,v)$.

Theorem 7.1. *Spline $B_{0,0,0}(u,v)$ is*

$$B_{0,0,0}(u,v)=\begin{cases}2(1+v)^2, & (u,v)\in D_1\\ 2+4v-u^2-4uv-2v^2, & (u,v)\in D_2\\ (2-u)^2, & (u,v)\in D_3\\ 2(1-v)^2, & (u,v)\in D_4\\ 1+2u-u^2-4uv-2v^2, & (u,v)\in D_5\\ (1+u)^2, & (u,v)\in D_6\\ 1+2u-u^2+4uv-2v^2, & (u,v)\in D_7\\ 2-4v-u^2+4uv-2v^2, & (u,v)\in D_8\\ 1+2u-2u^2-6v^2, & (u,v)\in D_9\\ 0, & \textit{otherwise},\end{cases} \tag{7.2}$$

where D_i is still shown in Fig. 3, but the u-coordinates of the points in Fig. 3 should be decreased by 1. The support for $B_{0,0,0}(u,v)$ is $[-1,2]\times[-1,1]$.

Proof. Since $B_{1,0,0}(u,v)=B_{0,0,0}(u-1,v)$, formula (7.2) is derived from formula (7.1) in Lemma 7.1. □

https://doi.org/10.4208/nmtma.2016.y14020 Published online by Cambridge University Press

Theorem 7.2. *Spline* $B_{0,0,1}(u,v)$ *is*

$$B_{0,0,1}(u,v)=\begin{cases}2(1+u)^2, & (u,v)\in D_1'\\ 2+4u-v^2-4uv-2u^2, & (u,v)\in D_2'\\ (2-v)^2, & (u,v)\in D_3'\\ 2(1-u)^2, & (u,v)\in D_4'\\ 1+2v-v^2-4uv-2u^2, & (u,v)\in D_5'\\ (1+v)^2, & (u,v)\in D_6'\\ 1+2v-v^2+4uv-2u^2, & (u,v)\in D_7'\\ 2-4u-v^2+4uv-2u^2, & (u,v)\in D_8'\\ 1+2v-2v^2-6u^2, & (u,v)\in D_9'\\ 0, & \textit{otherwise},\end{cases} \tag{7.3}$$

where D_i' *are symmetric sets of* D_i *in (7.2), or exactly,* $D_i'=\{(u,v):(v,u)\in D_i\}$. *The support for* $B_{0,0,1}(u,v)$ *is* $[-1,1]\times[-1,2]$.

Proof. $B_{0,0,1}(u,v)=B_{0,0,0}(v,u)$ by Lemma 6.2. Together with formula (7.2), formula (7.3) follows. □

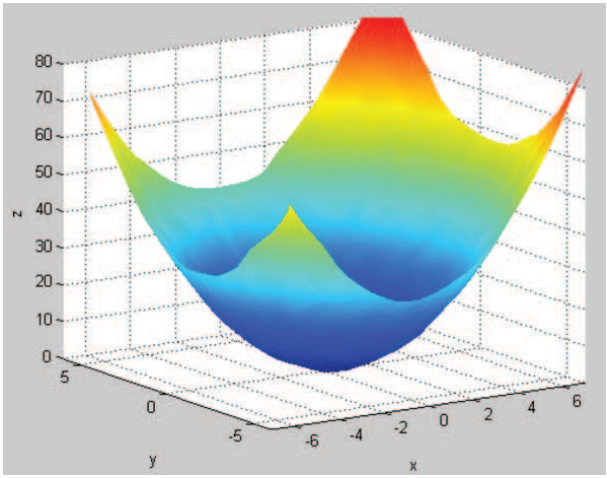


Figure 5: A bivariate quadratic spline surface with random control points.

Based on Eqs. (7.2) and (7.3), 12 functions $\{M_{i,j,k}(u,v):(i,j,k)\in \mathbb{D}_{0,0}\}$ in Eq. (6.5) can be derived directly. Similar functions are analysed in [12] in detail.

Fig. 5 is a bivariate C^1-quadratic spline surface [12] with constant weights and

https://doi.org/10.4208/nmtma.2016.y14020 Published online by Cambridge University Press

control points $P_{i,j,k} = (x_{i,j,k}, y_{i,j,k}, z_{i,j,k})$:

$$\begin{cases} x_{i,j,0} = i + 0.5 + \text{rand}(1,15), & i = -7, ..., 7, \\ y_{i,j,0} = j + \text{rand}(1,13), & j = -6, ..., 6, \\ x_{i,j,1} = i + \text{rand}(1,14), & i = -6, ..., 7, \\ y_{i,j,1} = j + 0.5 + \text{rand}(1,14), & j = -7, ..., 6, \\ z_{i,j,k} = x_{i,j,k}^2 + y_{i,j,k}^2. \end{cases}$$

where $\text{rand}(\cdot,\cdot)$ is a random function in MatLab.

8. Bivariate quadratic spline patch boundary properties

Boundary properties of patch $P_{m,n}(u,v)$ in Eq. (6.5) are analysed below.

Corollary 8.1. *$P_{m,n}(u,v)$ is generated by only 12 control points $P_{i,j,k}, (i,j,k) \in \mathbb{D}_{mn}$. These 12 control points are topologically distributed in Fig. 6.*

Proof. Corollary 8.1 is direct by Theorem 6.1 and formula (6.5). □

It is evident that $P_{m,n}(u,v)$ is in rational form. Let's denote its numerator and denominator as $A_{m,n}(u,v)$ and $B_{m,n}(u,v)$, respectively. Then we have the following functions:

Lemma 8.1. *$P_{m,n}(u,v)$ in Eq. (6.5) and its numerator and denominator, $A_{m,n}(u,v)$ and $B_{m,n}(u,v)$, satisfy*

$$\begin{cases} A_{m,n}(u,v) = \displaystyle\sum_{(i,j,k)\in\mathbb{D}_{0,0}} \omega_{i+m,j+n,k} B_{i,j,k}(u,v) P_{i+m,j+n,k}, \\ B_{m,n}(u,v) = \displaystyle\sum_{(i,j,k)\in\mathbb{D}_{0,0}} \omega_{i+m,j+n,k} B_{i,j,k}(u,v), \\ P_{m,n}(u,v) = \dfrac{A_{m,n}(u,v)}{B_{m,n}(u,v)}, \qquad (u,v) \in [0,1] \times [0,1]. \end{cases} \tag{8.1}$$

And, their partial derivatives satisfy

$$\begin{cases} A_{m,n}^u(u,v) \equiv \dfrac{\partial A_{m,n}(u,v)}{\partial u}, \quad A_{m,n}^v(u,v) \equiv \dfrac{\partial A_{m,n}(u,v)}{\partial v}, \\ B_{m,n}^u(u,v) \equiv \dfrac{\partial B_{m,n}(u,v)}{\partial u}, \quad B_{m,n}^v(u,v) \equiv \dfrac{\partial B_{m,n}(u,v)}{\partial v}, \\ P_{m,n}^u(u,v) \equiv \dfrac{\partial P_{m,n}(u,v)}{\partial u} \\ \qquad = \dfrac{A_{m,n}^u(u,v) B_{m,n}(u,v) - A_{m,n}(u,v) B_{m,n}^u(u,v)}{B_{m,n}^2(u,v)}, \\ P_{m,n}^v(u,v) \equiv \dfrac{\partial P_{m,n}(u,v)}{\partial v} \\ \qquad = \dfrac{A_{m,n}^v(u,v) B_{m,n}(u,v) - A_{m,n}(u,v) B_{m,n}^v(u,v)}{B_{m,n}^2(u,v)}. \end{cases} \tag{8.2}$$

https://doi.org/10.4208/nmtma.2016.y14020 Published online by Cambridge University Press

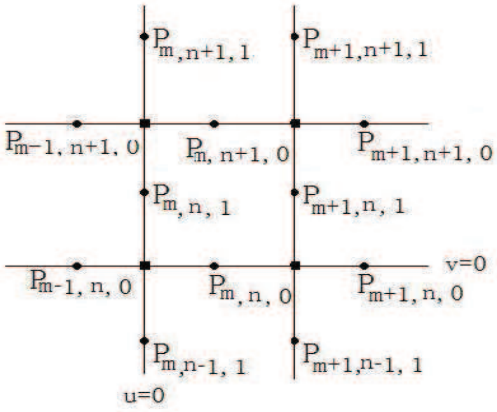


Figure 6: Topological distribution of control points of $P_{m,n}(u,v)$ in formula (6.5).

Lemma 8.2 is presented in [12].

Lemma 8.2. *The boundary curve of* $P_{0,0}(u,v) = A_{0,0}(u,v)/B_{0,0}(u,v)$ *along line* $v = 0$ *satisfies*

$$A_{0,0}(u,0) = \begin{cases} \omega_{-1,0,0}P_{-1,0,0}(u^2-2u+1) + \omega_{0,0,0}P_{0,0,0}(-2u^2+2u+1) \\ +\omega_{1,0,0}P_{1,0,0}u^2 + \omega_{0,0,1}P_{0,0,1}(-2u^2+1) + \omega_{0,-1,1}P_{0,-1,1}(-2u^2+1) \\ +2\omega_{1,0,1}P_{1,0,1}u^2 + 2\omega_{1,-1,1}P_{1,-1,1}u^2, \qquad u \in [0,0.5), \\ \omega_{-1,0,0}P_{-1,0,0}(u^2-2u+1) + \omega_{0,0,0}P_{0,0,0}(-2u^2+2u+1) \\ +\omega_{1,0,0}P_{1,0,0}u^2 + \omega_{0,0,1}P_{0,0,1}(2u^2-4u+2) \\ +\omega_{0,-1,1}P_{0,-1,1}(2u^2-4u+2) + \omega_{1,0,1}P_{1,0,1}(-2u^2+4u-1) \\ +\omega_{1,-1,1}P_{1,-1,1}(-2u^2+4u-1), \qquad u \in [0.5,1], \end{cases} \tag{8.3}$$

$$B_{0,0}(u,0) = \begin{cases} \omega_{-1,0,0}(u^2-2u+1) + \omega_{0,0,0}(-2u^2+2u+1) \\ +\omega_{1,0,0}u^2 + \omega_{0,0,1}(-2u^2+1) + \omega_{0,-1,1}(-2u^2+1) \\ +2\omega_{1,0,1}u^2 + 2\omega_{1,-1,1}u^2, \qquad u \in [0,0.5), \\ \omega_{-1,0,0}(u^2-2u+1) + \omega_{0,0,0}(-2u^2+2u+1) \\ +\omega_{1,0,0}u^2 + \omega_{0,0,1}(2u^2-4u+2) \\ +\omega_{0,-1,1}(2u^2-4u+2) + \omega_{1,0,1}(-2u^2+4u-1) \\ +\omega_{1,-1,1}(-2u^2+4u-1), \qquad u \in [0.5,1]. \end{cases} \tag{8.4}$$

Corollary 8.2. *The boundary curve of* $P_{m,n}(u,v) = A_{m,n}(u,v)/B_{m,n}(u,v)$ *along line*

https://doi.org/10.4208/nmtma.2016.y14020 Published online by Cambridge University Press

$v = 0$ *satisfies*

$$A_{m,n}(u,0) = \begin{cases} \omega_{m-1,n,0}P_{m-1,n,0}(1-u)^2 \\ +(\omega_{m,n-1,1}P_{m,n-1,1} + \omega_{m,n,1}P_{m,n,1})(1-2u^2) \\ +\omega_{m,n,0}P_{m,n,0}(1+2u(1-u)) \\ +(\omega_{m+1,n-1,1}P_{m+1,n-1,1} + \omega_{m+1,n,1}P_{m+1,n,1})(2u^2) \\ +\omega_{m+1,n,0}P_{m+1,n,0}u^2, & u \in [0, 0.5), \\ \omega_{m-1,n,0}P_{m-1,n,0}(1-u)^2 \\ +(\omega_{m,n-1,1}P_{m,n-1,1} + \omega_{m,n,1}P_{m,n,1})(2(1-u)^2) \\ +\omega_{m,n,0}P_{m,n,0}(1+2u(1-u)) \\ +(\omega_{m+1,n,1}P_{m+1,n,1} \\ \qquad +\omega_{m+1,n-1,1}P_{m+1,n-1,1})(1-2(1-u)^2) \\ +\omega_{m+1,n,0}P_{m+1,n,0}u^2, & u \in [0.5, 1], \end{cases} \tag{8.5}$$

$$B_{m,n}(u,0) = \begin{cases} \omega_{m-1,n,0}(1-u)^2 + (\omega_{m,n-1,1} + \omega_{m,n,1})(1-2u^2) \\ +\omega_{m,n,0}(1+2u(1-u)) + (\omega_{m+1,n-1,1} + \omega_{m+1,n,1})(2u^2) \\ +\omega_{m+1,n,0}u^2, & u \in [0, 0.5), \\ \omega_{m-1,n,0}(1-u)^2 + (\omega_{m,n-1,1} + \omega_{m,n,1})(2(1-u)^2) \\ +\omega_{m,n,0}(1+2u(1-u)) \\ +(\omega_{m+1,n,1} + \omega_{m+1,n-1,1})(1-2(1-u)^2) \\ +\omega_{m+1,n,0}u^2, & u \in [0.5, 1]. \end{cases} \tag{8.6}$$

Proof. Based on Eq. (6.5), the expressions of $P_{m,n}(u,v)$ and $P_{0,0}(u,v)$ are similar. Hence, the boundary curve of $P_{m,n}(u,v) = A_{m,n}(u,v)/B_{m,n}(u,v)$ along line $v = 0$ can be deduced from Eqs. (8.3) and (8.4) in Lemma 8.2. □

As shown in Fig. 6, only the 7 control points along line $v = 0$ and their weights are involved in Eq. (8.5), and only the weights related to those 7 control points are involved in Eq. (8.6).

For the other three boundary curves of $P_{m,n}(u,v) = A_{m,n}(u,v)/B_{m,n}(u,v)$ along line $u = 0$, $v = 1$ and $u = 1$, the related functions can be derived similarly.

Theorem 8.1. *If $\omega_{i,j,k}$ are positive constants, the four boundary curves of rational quadratic spline patch $P_{m,n}(u,v) = A_{m,n}(u,v)/B_{m,n}(u,v)$ are piecewise quadratic polynomial curves.*

Proof. If $\omega_{i,j,k} = c$(constant), by Eq. (8.6),

$$B_{m,n}(u,0) = c((1-u)^2 + (1-2u^2) + (1+2u(1-u)) + (2u^2) + u^2) \equiv 3c$$

for $0 \le u \le 0.5$, and

$$B_{m,n}(u,0) = c((1-u)^2 + 2(1-u)^2 + (1+2u(1-u)) + (1-2(1-u)^2) + u^2) \equiv 3c$$

for $0.5 \le u \le 1$. $B_{m,n}(u,0) \equiv 3c$ is a constant for $0 \le u \le 1$, however. Similarly,

$$B_{m,n}(0,v) \equiv B_{m,n}(u,1) \equiv B_{m,n}(1,v) \equiv 3c$$

https://doi.org/10.4208/nmtma.2016.y14020 Published online by Cambridge University Press

are constants for $0 \le u \le 1$ or $0 \le v \le 1$. And the conclusions follow. □

Now, let us analyse the tangent vectors along the boundary curves of $P_{m,n}(u,v) = A_{m,n}(u,v)/B_{m,n}(u,v)$.

For the $v-$directional vectors across boundary curve along line $v = 0$,

$$A^v_{m,n}(u,0) = \begin{cases} \omega_{m,n,1}P_{m,n,1}(2-4u) \\ +\omega_{m,n-1,1}P_{m,n-1,1}(-2+4u), & u \in [0,0.5], \\ \omega_{m+1,n,1}P_{m+1,n,1}(-2+4u) \\ +\omega_{m+1,n-1,1}P_{m+1,n-1,1}(2-4u), & u \in (0.5,1], \end{cases} \tag{8.7}$$

$$B^v_{m,n}(u,0) = \begin{cases} \omega_{m,n,1}(2-4u) + \omega_{m,n-1,1}(-2+4u), & u \in [0,0.5], \\ \omega_{m+1,n,1}(-2+4u) + \omega_{m+1,n-1,1}(2-4u), & u \in (0.5,1]. \end{cases} \tag{8.8}$$

Hence,

$$\frac{A^v_{m,n}(u,0)}{2|1-2u|} = \begin{cases} \omega_{m,n,1}P_{m,n,1} - \omega_{m,n-1,1}P_{m,n-1,1}, & u \in [0,0.5], \\ \omega_{m+1,n,1}P_{m+1,n,1} - \omega_{m+1,n-1,1}P_{m+1,n-1,1}, & u \in (0.5,1], \end{cases} \tag{8.9}$$

$$B^v_{m,n}(u,0)/(2|1-2u|) = \begin{cases} \omega_{m,n,1} - \omega_{m,n-1,1}, & u \in [0,0.5], \\ \omega_{m+1,n,1} - \omega_{m+1,n-1,1}, & u \in (0.5,1], \end{cases} \tag{8.10}$$

and $v-$directional tangent vector function

$$\begin{aligned} & P^v_{m,n}(u,0)[B_{m,n}(u,0)]^2/(2|1-2u|) \\ &= (A^v_{m,n}(u,0)B_{m,n}(u,0) - A_{m,n}(u,0)B^v_{m,n}(u,0))/(2|1-2u|) \\ &= \begin{cases} \omega_{m,n,1}(P_{m,n,1}B_{m,n}(u,0) - A_{m,n}(u,0)) \\ \quad +\omega_{m,n-1,1}(A_{m,n}(u,0) - P_{m,n-1,1}B_{m,n}(u,0)), & u \in [0,0.5), \\ \omega_{m+1,n,1}(P_{m+1,n,1}B_{m,n}(u,0) - A_{m,n}(u,0)) \\ \quad +\omega_{m+1,n-1,1}(A_{m,n}(u,0) - P_{m+1,n-1,1}B_{m,n}(u,0)), & u \in [0.5,1]. \end{cases} \end{aligned} \tag{8.11}$$

The 4 terms in (8.11) are similar and are expanded as follows.

$$\begin{aligned} & \omega_{m,n,1}(P_{m,n,1}B_{m,n}(u,0) - A_{m,n}(u,0)) \\ &= \begin{cases} \omega_{m-1,n,0}\omega_{m,n,1}(P_{m,n,1} - P_{m-1,n,0})(1-u)^2 \\ \quad +\omega_{m,n-1,1}\omega_{m,n,1}(P_{m,n,1} - P_{m,n-1,1})(1-2u^2) \\ \quad +\omega_{m,n,0}\omega_{m,n,1}(P_{m,n,1} - P_{m,n,0})(1+2u(1-u)) \\ \quad +[2\omega_{m+1,n-1,1}\omega_{m,n,1}(P_{m,n,1} - P_{m+1,n-1,1}) \\ \quad +2\omega_{m+1,n,1}\omega_{m,n,1}(P_{m,n,1} - P_{m+1,n,1}) \\ \quad +\omega_{m+1,n,0}\omega_{m,n,1}(P_{m,n,1} - P_{m+1,n,0})]u^2, & u \in [0,0.5), \end{cases} \end{aligned} \tag{8.12}$$

https://doi.org/10.4208/nmtma.2016.y14020 Published online by Cambridge University Press

$$
\begin{aligned}
&\omega_{m,n-1,1}(A_{m,n}(u,0)-P_{m,n-1,1}B_{m,n}(u,0)))\\
&=\begin{cases}
\omega_{m-1,n,0}\omega_{m,n-1,1}(P_{m-1,n,0}-P_{m,n-1,1})(1-u)^2\\
\quad+\omega_{m,n,1}\omega_{m,n-1,1}(P_{m,n,1}-P_{m,n-1,1})(1-2u^2)\\
\quad+\omega_{m,n,0}\omega_{m,n-1,1}(P_{m,n,0}-P_{m,n-1,1})(1+2u(1-u))\\
\quad+[2\omega_{m+1,n-1,1}\omega_{m,n-1,1}(P_{m+1,n-1,1}-P_{m,n-1,1})\\
\quad+2\omega_{m+1,n,1}\omega_{m,n-1,1}(P_{m+1,n,1}-P_{m,n-1,1})\\
\quad+\omega_{m+1,n,0}\omega_{m,n-1,1}(P_{m+1,n,0}-P_{m,n-1,1})]u^2, \qquad u\in[0,0.5),
\end{cases}
\end{aligned}
\tag{8.13}
$$

$$
\begin{aligned}
&\omega_{m+1,n,1}(P_{m+1,n,1}B_{m,n}(u,0)-A_{m,n}(u,0))\\
&=\begin{cases}
[\omega_{m-1,n,0}\omega_{m+1,n,1}(P_{m+1,n,1}-P_{m-1,n,0})\\
\quad+2\omega_{m,n-1,1}\omega_{m+1,n,1}(P_{m+1,n,1}-P_{m,n-1,1})\\
\quad+2\omega_{m,n,1}\omega_{m+1,n,1}(P_{m+1,n,1}-P_{m,n,1})](1-u)^2\\
\quad+\omega_{m,n,0}\omega_{m+1,n,1}(P_{m+1,n,1}-P_{m,n,0})(1+2u(1-u))\\
\quad+\omega_{m+1,n-1,1}\omega_{m+1,n,1}(P_{m+1,n,1}-P_{m+1,n-1,1})(1-2(1-u)^2)\\
\quad+\omega_{m+1,n,0}\omega_{m+1,n,1}(P_{m+1,n,1}-P_{m+1,n,0})u^2, \qquad u\in[0.5,1],
\end{cases}
\end{aligned}
\tag{8.14}
$$

$$
\begin{aligned}
&\omega_{1,-1,1}(A_{m,n}(u,0)-P_{1,-1,1}B_{m,n}(u,0))\\
&=\begin{cases}
[\omega_{m-1,n,0}\omega_{m+1,n-1,1}(P_{m-1,n,0}-P_{m+1,n-1,1})\\
\quad+2\omega_{m,n-1,1}\omega_{m+1,n-1,1}(P_{m,n-1,1}-P_{m+1,n-1,1})\\
\quad+2\omega_{m,n,1}\omega_{m+1,n-1,1}(P_{m,n,1}-P_{m+1,n-1,1})](1-u)^2\\
\quad+\omega_{m,n,0}\omega_{m+1,n-1,1}(P_{m,n,0}-P_{m+1,n-1,1})(1+2u(1-u))\\
\quad+\omega_{m+1,n,1}\omega_{m+1,n-1,1}(P_{m+1,n,1}-P_{m+1,n-1,1})(1-2(1-u)^2)\\
\quad+\omega_{m+1,n,0}\omega_{m+1,n-1,1}(P_{m+1,n,0}-P_{m+1,n-1,1})u^2, \qquad u\in[0.5,1].
\end{cases}
\end{aligned}
\tag{8.15}
$$

Vectors involved in equations from (8.12) to (8.15) are shown in Fig. 6. By the scripts of the control points involved in those equations, the $v-$directional tangent vector is a linear combination of the vectors which are difference of the control points along the boundary.

As for the $u-$directional tangent vector along the boundary, it can be seen from (8.5) and (8.6) that

https://doi.org/10.4208/nmtma.2016.y14020 Published online by Cambridge University Press

$$A^u_{m,n}(u,0)=\begin{cases}(\omega_{m+1,n,0}P_{m+1,n,0}-\omega_{m,n,0}P_{m,n,0})(2u)\\ \quad+(\omega_{m,n,0}P_{m,n,0}-\omega_{m-1,n,0}P_{m-1,n,0})(2(1-u))\\ \quad+[(\omega_{m+1,n,1}P_{m+1,n,1}-\omega_{m,n,1}P_{m,n,1})\\ \quad+(\omega_{m+1,n-1,1}P_{m+1,n-1,1}-\omega_{m,n-1,1}P_{m,n-1,1})](4u)\\ \qquad\qquad\qquad\qquad\qquad\qquad u\in[0,0.5],\\ (\omega_{m+1,n,0}P_{m+1,n,0}-\omega_{m,n,0}P_{m,n,0})(2u)\\ \quad+(\omega_{m,n,0}P_{m,n,0}-\omega_{m-1,n,0}P_{m-1,n,0})(2(1-u))\\ \quad+[(\omega_{m+1,n,1}P_{m+1,n,1}-\omega_{m,n,1}P_{m,n,1})\\ \quad+(\omega_{m+1,n-1,1}P_{m+1,n-1,1}-\omega_{m,n-1,1}P_{m,n-1,1})](4(1-u))\\ \qquad\qquad\qquad\qquad\qquad\qquad u\in(0.5,1],\end{cases}\tag{8.16}$$

$$B^u_{m,n}(u,0)=\begin{cases}(\omega_{m+1,n,0}-\omega_{m,n,0})(2u)\\ \quad+(\omega_{m,n,0}-\omega_{m-1,n,0})(2(1-u))\quad+[(\omega_{m+1,n,1}-\omega_{m,n,1})\\ \quad+(\omega_{m+1,n-1,1}-\omega_{m,n-1,1})](4u)\qquad u\in[0,0.5],\\ (\omega_{m+1,n,0}-\omega_{m,n,0})(2u)\\ \quad+(\omega_{m,n,0}-\omega_{m-1,n,0})(2(1-u))\quad+[(\omega_{m+1,n,1}-\omega_{m,n,1})\\ \quad+(\omega_{m+1,n-1,1}-\omega_{m,n-1,1})](4(1-u))\qquad u\in(0.5,1].\end{cases}\tag{8.17}$$

Actually, the expression of vector

$$P^u_{m,n}(u,0)[B_{m,n}(u,0)]^2=A^u_{m,n}(u,0)B_{m,n}(u,0)-A_{m,n}(u,0)B^u_{m,n}(u,0)\tag{8.18}$$

is similar to that of $P^v_{m,n}(u,0)[B_{m,n}(u,0)]^2$ which is expressed in Eq. (8.11) with the results in equations from (8.12) to (8.15). The control points involved in $P^u_{m,n}(u,0)$ are shown in Fig. 6. Based on the scripts of these control points, the $u-$directional tangent vector along this boundary curve is a linear combination of the vectors which are difference of the control points along the boundary.

The tangent vectors for the other boundary curves of $P_{m,n}(u,v)$ along line $u=0$, $v=1$ and $u=1$ can be derived analogously.

Let $Q_{m,n}(u,v)$ be a patch similar to $P_{m,n}(u,v)$, and the related control points and weights are $Q_{i,j,k}$ and $w_{i,j,k}$. Intuitively, $Q_{m,n}(u,v)$ in the sense of equation (6.11) can be considered as another patch below $P_{m,n}(u,v)$.

Associated with formulas of boundary curves and their tangents, we have

Theorem 8.2. *Two patches, $P_{0,0}(u,v)$ along $v=0$ and $Q_{0,0}(u,v)$ along $v=1$, are C^1-connected if the control points $P_{i,j,k}$ and weights $\omega_{i,j,k}$ along $v=0$ coincide with the control points $Q_{i,j,k}$ and weights $w_{i,j,k}$ along $v=1$, that is:*

$$P_{i,j,k}=Q_{i,j+1,k},\omega_{i,j,k}=w_{i,j+1,k},\ \textit{for}\ \ (i,j,k)\in I\!D_{.0},\tag{8.19}$$

where

$$I\!D_{.0}=\{(-1,0,0),(0,0,0),(1,0,0),(0,0,1),(0,-1,1),(1,0,1),(1,-1,1)\}\tag{8.20}$$

https://doi.org/10.4208/nmtma.2016.y14020 Published online by Cambridge University Press

Proof. If Eq. (8.19) holds, patch $Q_{0,0}(u,v)$ in Theorem 8.2 can be considered as patch $P_{0,-1}(u,v)$ and its control points and weights as that of $P_{0,-1}(u,v)$. As two adjacent patches of C^1-surface $P(u,v)$, $P_{0,0}(u,v)$ and $P_{0,-1}(u,v)$ along $v=0$ are C^1-connected. That is, $P_{0,0}(u,v)$ along $v=0$ and $Q_{0,0}(u,v)$ along $v=1$, are C^1-connected. □

9. Bivariate quadratic spline patch corner properties

Theorem 9.1. *The 4 conner points of patch* $P_{m,n}(u,v)$ *in Eq.* (6.5) *are:*

$$\begin{cases} P_{m,n}(0,0) = \dfrac{\sum\limits_{(i,j,k)\in \mathbb{D}_q} \omega_{m+i,n+j,k} P_{m+i,n+j,k}}{\sum\limits_{(i,j,k)\in \mathbb{D}_q} \omega_{m+i,n+j,k}}, \\ P_{m,n}(1,0) = \dfrac{\sum\limits_{(i,j,k)\in \mathbb{D}_q} \omega_{m+1+i,n+j,k} P_{m+1+i,n+j,k}}{\sum\limits_{(i,j,k)\in \mathbb{D}_q} \omega_{m+1+i,n+j,k}}, \\ P_{m,n}(0,1) = \dfrac{\sum\limits_{(i,j,k)\in \mathbb{D}_q} \omega_{m+i,n+1+j,k} P_{m+i,n+1+j,k}}{\sum\limits_{(i,j,k)\in \mathbb{D}_q} \omega_{m+i,n+1+j,k}}, \\ P_{m,n}(1,1) = \dfrac{\sum\limits_{(i,j,k)\in \mathbb{D}_q} \omega_{m+1+i,n+1+j,k} P_{m+1+i,n+1+j,k}}{\sum\limits_{(i,j,k)\in \mathbb{D}_q} \omega_{m+1+i,n+1+j,k}}, \end{cases} \tag{9.1}$$

where

$$\mathbb{D}_q = \{(-1,0,0),(0,-1,1),(0,0,0),(0,0,1)\}, \tag{9.2}$$

Proof. From Eqs. (8.5) and (8.6), we have

$$\begin{cases} A_{m,n}(0,0) = \omega_{m-1,n,0} P_{m-1,n,0} + \omega_{m,n,0} P_{m,n,0} \\ \qquad\qquad +\omega_{m,n,1} P_{m,n,1} + \omega_{m,n-1,1} P_{m,n-1,1}, \\ A_{m,n}(1,0) = \omega_{m,n,0} P_{m,n,0} + \omega_{m+1,n,0} P_{m+1,n,0} \\ \qquad\qquad +\omega_{m+1,n,1} P_{m+1,n,1} + \omega_{m+1,n-1,1} P_{m+1,n-1,1}, \end{cases} \tag{9.3}$$

$$\begin{cases} B_{m,n}(0,0) = \omega_{m-1,n,0} + \omega_{m,n,0} + \omega_{m,n,1} + \omega_{m,n-1,1}, \\ B_{m,n}(1,0) = \omega_{m,n,0} + \omega_{m+1,n,0} + \omega_{m+1,n,1} + \omega_{m+1,n-1,1}. \end{cases} \tag{9.4}$$

With $\mathbb{D}_q$ in formula (9.2), we have

$$\begin{cases} A_{m,n}(0,0) = \sum\limits_{(i,j,k)\in \mathbb{D}_q} \omega_{m+i,n+j,k} P_{m+i,n+j,k}, \\ A_{m,n}(1,0) = \sum\limits_{(i,j,k)\in \mathbb{D}_q} \omega_{m+1+i,n+j,k} P_{m+1+i,n+j,k}, \end{cases} \tag{9.5}$$

https://doi.org/10.4208/nmtma.2016.y14020 Published online by Cambridge University Press

$$B_{m,n}(0,0)=\sum_{(i,j,k)\in\mathbb{D}_q}\omega_{m+i,n+j,k},\ B_{m,n}(1,0)=\sum_{(i,j,k)\in\mathbb{D}_q}\omega_{m+1+i,n+j,k}. \tag{9.6}$$

Analogously,

$$\begin{cases} A_{m,n}(0,1)=\sum\limits_{(i,j,k)\in\mathbb{D}_q}\omega_{m+i,n+1+j,k}P_{m+i,n+1+j,k},\\ A_{m,n}(1,1)=\sum\limits_{(i,j,k)\in\mathbb{D}_q}\omega_{m+1+i,n+1+j,k}P_{m+1+i,n+1+j,k}, \end{cases} \tag{9.7}$$

$$B_{m,n}(0,1)=\sum_{(i,j,k)\in\mathbb{D}_q}\omega_{m+i,n+1+j,k},\ B_{m,n}(1,1)=\sum_{(i,j,k)\in\mathbb{D}_q}\omega_{m+1+i,n+1+j,k}. \tag{9.8}$$

Since $P_{m,n}(u,v)=A_{m,n}(u,v)/B_{m,n}(u,v)$, formula (9.1) follows. □

As shown in Fig. 6, the ordered 4 control points $\{P_{m+i,n+j,k}:(i,j,k)\in\mathbb{D}_q\}$ form a 3-Dimensional quadrilateral. This quadrilateral is a (corner) quadrilateral around a corner point of $P_{m,n}(u,v)$ consisting of the 4 control points around the corner point.

Corollary 9.1. *1) A corner point of $P_{m,n}(u,v)$ is the weighted average of the related 4 corner control points. If the related weights are constant, a corner point of $P_{m,n}(u,v)$ is the barycentric point of the related 4 corner control points.*

2) If the related 4 control points around a corner point are coplanar, the corner point of $P_{m,n}(u,v)$ is on the plane.

Proof. Corollary 9.1 is a direct result from Eq. (9.1). The mathematical details are ommitted. □

Based on Eq. (8.11), the $v-$directional tangent vector at corner point $P_{m,n}(0,0)$ is

$$\begin{aligned} P^v_{m,n}(0,0)=\frac{2}{[B_{m,n}(0,0)]^2}\Big(&2\omega_{m,n,1}\omega_{m,n-1,1}(P_{m,n,1}-P_{m,n-1,1})\\ &+\omega_{m,n,1}\omega_{m-1,n,0}(P_{m,n,1}-P_{m-1,n,0})\\ &+\omega_{m-1,n,0}\omega_{m,n-1,1}(P_{m-1,n,0}-P_{m,n-1,1})\\ &+\omega_{m,n,1}\omega_{m,n,0}(P_{m,n,1}-P_{m,n,0})+\omega_{m,n,0}\omega_{m,n-1,1}(P_{m,n,0}-P_{m,n-1,1})\Big), \end{aligned} \tag{9.9}$$

where $B_{m,n}(0,0)$ is expressed in (9.6). The first term of $P^v_{m,n}(0,0)$ is the $v-$directional diagonal vector of the related corner quadrilateral, the other four terms are the four $v-$directional edge vectors of the related corner quadrilateral.

Similarly, the $u-$directional tangent vector at corner point $P_{m,n}(0,0)$ is

$$\begin{aligned} P^u_{m,n}(0,0)=&\frac{2}{[B_{m,n}(0,0)]^2}\Big(2\omega_{m,n,0}\omega_{m-1,n,0}(P_{m,n,0}-P_{m-1,n,0})\\ &+\omega_{m,n,0}\omega_{m,n,1}(P_{m,n,0}-P_{m,n,1})+\omega_{m,n,1}\omega_{m-1,n,0}(P_{m,n,1}-P_{m-1,n,0})\\ &+\omega_{m,n,0}\omega_{m,n-1,1}(P_{m,n,0}-P_{m,n-1,1})\\ &+\omega_{m-1,n,0}\omega_{m-1,n,1}(P_{m,n-1,1}-P_{m-1,n,0})\Big). \end{aligned} \tag{9.10}$$

https://doi.org/10.4208/nmtma.2016.y14020 Published online by Cambridge University Press

The first term of $P^u_{m,n}(0,0)$ is the $u-$directional diagonal vector of the related corner quadrilateral, the other four terms are the four $u-$directional edge vectors of the related corner quadrilateral.

The directional tangent vectors at the other corner points of $P^u_{m,n}(u,v)$ can be derived analogously.

Corollary 9.2. 1) *The directional tangent vectors at the corner points of $P_{m,n}(u,v)$ is linear combinations of the related directional diagonal and* 4 *edges vectors in the corner quadrilateral.*

2) *If the related* 4 *control points around a corner point of $P_{m,n}(u,v)$ are coplanar, this plane is the tangent plane at the corner.*

3) *If the related* 4 *weights around a corner point of $P_{m,n}(u,v)$ are constants, the two directional tangent vectors at the corner are halves of the two diagonal vectors.*

Proof. 1) and 2) are direct results from Corollary 9.1, equations (9.9) and (9.10).

3) can be derived as follows. If the related 4 weights around a corner point $P_{m,n}(0,0)$ are constants, let the related weights $\omega_{i,j,k} = c$.

Based on Eq. (9.9), the $v-$directional tangent vector at corner point $P_{m,n}(0,0)$ is

$$\begin{aligned} P^v_{m,n}(0,0) =& \frac{2c^2}{[B_{m,n}(0,0)]^2}[2(P_{m,n,1} - P_{m,n-1,1}) + (P_{m,n,1} - P_{m-1,n,0}) \\ &+ (P_{m-1,n,0} - P_{m,n-1,1}) + (P_{m,n,1} - P_{m,n,0}) + (P_{m,n,0} - P_{m,n-1,1})] \\ =& \frac{1}{2}(P_{m,n,1} - P_{m,n-1,1}), \end{aligned} \tag{9.11}$$

the half of one diagonal vector. Based on Eq. (9.10), the $u-$directional tangent vector at corner point $P_{m,n}(0,0)$ is

$$P^u_{m,n}(0,0) = \frac{1}{2}(P_{m,n,0} - P_{m-1,n,0}), \tag{9.12}$$

the half of another diagonal vector. □

10. C^1-connection between two patches

Suppose patch $Q_{0,0}(u,v)$ is topologically below patch $P_{0,0}(u,v)$. Based on the relationship between the control points of $P_{0,0}(u,v)$ and that of $Q_{0,0}(u,v)$, these two patches can be C^1-continuously connected in 3 cases below.

Case 1) The control points of the two patches are independent

In this case, two patches $Q_{0,0}(u,v)$ and $P_{0,0}(u,v)$ are designed separately.

Theorem 10.1. *Two independent patches $Q_{0,0}(u,v)$ and $P_{0,0}(u,v)$ can be C^1-continuously connected along a curve $C(u), 0 \le u \le 1$ which satisfies* (10.1).

$$C(0) = P_0, C(0.5) = P_{0.5}, C(1) = P_1, \tag{10.1}$$

https://doi.org/10.4208/nmtma.2016.y14020 Published online by Cambridge University Press

Proof. Firstly, consider patch $Q_{0,0}(u,v)$ as $P_{0,-3}(u,v)$, and its control points and weights as that of $P_{0,-3}(u,v)$.

Secondly, add three new control points and their weights $\{P_{i,-1,0}, \omega_{i,-1,0} : i = -1,0,1\}$.

These three control points, together with all of control points for patches $P_{0,0}(u,v)$ and $P_{0,-3}(u,v)$, can be used to generate four patches $P_{0,j}(u,v), j = -3,-2,-1,0$.

With two patches $P_{0,j}(u,v), j = -2,-1$, $Q_{0,0}(u,v)$ and $P_{0,0}(u,v)$ are C^1- continuously connected together along common boundary curve $C(u)$:

$$C(u) \equiv P_{0,-1}(u,0) = A_{0,-1}(u,0)/B_{0,-1}(u,0). \tag{10.2}$$

Topologically, the three new control points and their weights are along the common boundary $C(u)$ between two patches $P_{0,j}(u,v), j = -2,-1$.

According to formula (10.1), the three new control points and their weights $\{P_{i,-1,0}, \omega_{i,-1,0} : i = -1,0,1\}$ are solved as follow.

By Eqs. (8.5) and (8.6), we have

$$\begin{aligned} P_{0.5} &= P_{0,-1}(0.5,0) \\ &= \frac{\begin{array}{l}\omega_{-1,-1,0}P_{-1,-1,0} + 2(\omega_{0,-2,1}P_{0,-2,1} + \omega_{0,-1,1}P_{0,-1,1}) + 6\omega_{0,-1,0}P_{0,-1,0} \\ +\omega_{1,-1,0}P_{1,-1,0} + 2(\omega_{1,-2,1}P_{1,-2,1} + \omega_{1,-1,1}P_{1,-1,1})\end{array}}{\begin{array}{l}\omega_{-1,-1,0} + 2(\omega_{0,-2,1} + \omega_{0,-1,1}) + 6\omega_{0,-1,0} \\ +\omega_{1,-1,0} + 2(\omega_{1,-2,1} + \omega_{1,-1,1})\end{array}}. \end{aligned} \tag{10.3}$$

By Eq. (9.1), we have

$$P_0 = P_{0,-1}(0,0) = \frac{\begin{array}{l}\omega_{-1,-1,0}P_{-1,-1,0} + \omega_{0,-2,1}P_{0,-2,1} \\ +\omega_{0,-1,0}P_{0,-1,0} + \omega_{0,-1,1}P_{0,-1,1}\end{array}}{\omega_{-1,-1,0} + \omega_{0,-2,1} + \omega_{0,-1,0} + \omega_{0,-1,1}}, \tag{10.4}$$

$$P_1 = P_{0,-1}(1,0) = \frac{\begin{array}{l}\omega_{0,-1,0}P_{0,-1,0} + \omega_{1,-2,1}P_{1,-2,1} \\ +\omega_{1,-1,0}P_{1,-1,0} + \omega_{1,-1,1}P_{1,-1,1}\end{array}}{\omega_{0,-1,0} + \omega_{1,-2,1} + \omega_{1,-1,0} + \omega_{1,-1,1}}. \tag{10.5}$$

Simplify linear Eqs. (10.3), (10.4) and (10.5) as

$$\begin{cases} \omega_{-1,-1,0}P_{-1,-1,0} + 6\omega_{0,-1,0}P_{0,-1,0} + \omega_{1,-1,0}P_{1,-1,0} = C_{0.5}, \\ \omega_{-1,-1,0}P_{-1,-1,0} + \omega_{0,-1,0}P_{0,-1,0} = C_0, \\ \omega_{0,-1,0}P_{0,-1,0} + \omega_{1,-1,0}P_{1,-1,0} = C_1, \end{cases} \tag{10.6}$$

where $C_{0.5}$, C_0, C_1 are known vectors, expressed as:

$$\begin{cases} C_{0.5} = P_{0.5,0}B_{0,-1}(0.5,0) - 2\omega_{0,-2,1}P_{0,-2,1} - 2\omega_{0,-1,1}P_{0,-1,1} \\ \qquad\qquad -2\omega_{1,-2,1}P_{1,-2,1} - 2\omega_{1,-1,1}P_{1,-1,1}, \\ C_0 = P_0B_{0,-1}(0,0) - \omega_{0,-2,1}P_{0,-2,1} - \omega_{0,-1,1}P_{0,-1,1}, \\ C_1 = P_1B_{0,-1}(1,0) - \omega_{1,-2,1}P_{1,-2,1} - \omega_{1,-1,1}P_{1,-1,1}. \end{cases} \tag{10.7}$$

https://doi.org/10.4208/nmtma.2016.y14020 Published online by Cambridge University Press

The solution of this linear equation (10.6) is

$$\begin{cases} P_{0,-1,0} = \dfrac{C_{0.5} - C_0 - C_1}{4\omega_{0,-1,0}}, \\ P_{-1,-1,0} = \dfrac{-C_{0.5} + 5C_0 + C_1}{4\omega_{-1,-1,0}}, \\ P_{1,-1,0} = \dfrac{-C_{0.5} + C_0 + 5C_1}{4\omega_{1,-1,0}}. \end{cases} \tag{10.8}$$

where the three weights, $\omega_{i,-1,0}, i = -1, 0, 1$, can be any positive values. □

Two endpoints of the common boundary $C(u)$, $C(0) = P_{0,-1}(0,0)$ and $C(1) = P_{0,-1}(1,0)$, are used to generate the curve position. The midpoint, $C(0.5) = P_{0,-1}(0.5,0)$, is used to move the curve up and down. If those three points on curve $C(u)$ are designed, $C(u)$ is fixed geometrically.

Case 2) The 2 bottom control points of $P_{0,0}(u,v)$ and 2 top control points of $Q_{0,0}(u,v)$ coincide, $i.e.$

$$P_{i,-1,1} = Q_{i,1,1}, \omega_{i,-1,1} = w_{i,1,1} : i = 0, 1. \tag{10.9}$$

About the geometrical relationship of the related control points, see Figure 6 as a reference. In this case, simply consider patch $Q_{0,0}(u,v)$ as $P_{0,-2}(u,v)$, and its control points and weights as that of $P_{0,-2}(u,v)$.

All of control points for patches $P_{0,0}(u,v)$ and $P_{0,-2}(u,v)$ can be used to generate three patches $P_{0,j}(u,v), j = -2, -1, 0$.

With patch $P_{0,-1}(u,v)$, $Q_{0,0}(u,v)$ and $P_{0,0}(u,v)$ are C^1- continuously connected together.

Case 3) The 7 bottom control points of $P_{0,0}(u,v)$ and 7 top control points of $Q_{0,0}(u,v)$ coincide, $i.e.$ Eq. (8.19) holds.

Based on Theorem 2.2, $Q_{0,0}(u,v)$ and $P_{0,0}(u,v)$ are C^1- continuously connected together.

11. Conclusion

C^{k-1}-tensor product NURBS surfaces are usually bi-k-order surfaces over uniform rectangular meshes. Actually, they are bivariate surfaces with total degree $2k$. In [6–8], C^1-surfaces over arbitrary meshes were generated by repairing the original meshes or control points in some senses. The degrees of those surfaces are greater than or equal to 4. Subdivision surfaces are usually continuous and can be C^1-continuous as limiting results. For $k = 1, 2, 3$, C^{k-1}-surfaces defined above are spline surfaces with degrees of k with locality and convex hull property.

As we know, there is a possible problem that plenty of NURBS surfaces could not be smoothly connected at a common point when they connect at this common point. For the spline surfaces defined above, this problem can disappear.

https://doi.org/10.4208/nmtma.2016.y14020 Published online by Cambridge University Press

Rational bivariate quadratic C^1-surfaces over rectangular mesh presented in details in sections from 6 to 10 demonstrate the validity of the theoretic results in sections from 2 to 5. The C^1-surfaces defined above are spline surfaces with degrees of 2 with locality and convex hull property. Further study for those splines and surfaces is next work in future.

References

[1] X.-K. Liang. Rational Qudratic B-spline Interpolation of Function Segments. Computation Mathematics, A Jounal of Chinese University (in Chinese), 2012,01:52–60.

[2] J. Xie, J.-Q. Tan and S.-F. Li. Quadratic Algebraic Hypobolic B-spline Curves with Weight Parameters. Computation Mathematics, A Jounal of Chinese University (in Chinese), 2011,04:337–346.

[3] L.-B. Jin and J.-S. Deng. Conversion Between (3,3,1,1) Hierarchical B-splines and Polynomial splines over Hierarchical T-meshes. Computatation Mathematics, A Jounal of Chinese University (in Chinese), 2009,04:330–342.

[4] L. Qin and L.-T. Guan. Minimal Surfaces Design Based on NURBS. Computatation Mathematics, A Jounal of Chinese University (in Chinese), 2005, S1:175–181.

[5] T. Goodman, Polyhedral Splines, in Computation of Curves and Surfaces, W. Dahmen, M. Gasca, and C.A. Micchelli, eds. Kluwer, Dordrecht, 1990, Springer Netherlands. pp: 347–382.

[6] Y.-C. Zhang, F.-P. Da and W.-Z. Song. Piecewise C^1 Surfaces Based on Bivariate Quartic Box-Splines for Arbitrary Triangular Meshes. Journal of Software, 2006, 17(10): 2211–2220.

[7] R.-Z. Feng and R.-H. Wang. Smooth spline surfaces over arbitrary topological triangular meshes. Journal of Software, 2003, 14(4):830–837.

[8] R.-R. Zhou, L.-Y. Zhang, X.-F. Pang and L.-S. Zhou. Smooth Piecewise Spline Surfaces over Arbitrary Control Polyhedron. Chinese Journal of Aeronautics, 2001, 14(1):57–64.

[9] C.-Y. Liu. Theory and application of Convex Curves and Surfaces in CAGD. ISBN 90-365-1577-7, Press of University of Twente, 2001.

[10] C.-Y. Liu and X.-P. Zhou. Research on Algorithm of Precision Modeling Body Surfaces in Electronic Ray-Tracing Technique. College Mathematics (in Chinese), 2014,30(6):34–38.

[11] Traas C. Practice of Bivariate Quadratic Simplicial Splines, in Computation of Curves and Surfaces, W. Dahmen, M. Gasca, and C.A. Micchelli, eds. Kluwer, Dordrecht, 1990, Springer Netherlands. pp:383-422

[12] W.-Y. Xu. The Construction and Application of the Bivariate Quadratic Splines on Uniform Rectangular Grids. Zhengzhou University, 2014.

[13] X.-J. Zhuang. The Construction and Application of the Bivariate Quadratic Spline Function Method In the Bezier Trianglar Mesh. Zhengzhou University, 2014.

https://doi.org/10.4208/nmtma.2016.y14020 Published online by Cambridge University Press